ETH zürich

PAUL SCHERRER INSTITUT

Muonic atom spectroscopy with radioactive targets

Stella Vogiatzi

On behalf of the muX collaboration*

17.10.2022

PSI2022: Physics of fundamental symmetries and interactions

* Institute of Nuclear Physics, Polish Academy of Sciences, Krakow, Poland | Paul Scherrer Institut, Villigen, Switzerland | ETH Zürich, Switzerland | Johannes Gutenberg University Mainz, Germany | KU Leuven, Belgium | GSI Helmholtzzentrum für Schwerionenforschung Darmstadt, Germany | Helmholtz Institute Mainz, Germany | Institut für Kernphysik, Universität zu Köln, Germany | LKB Paris, France | University of Groningen, The Netherlands | University of Pisa and INFN, Pisa, Italy | University of Victoria, Canada | Perimeter Institute, Waterloo, Canada | CSNSM, Université Paris Sud, CNRS/IN2P3, Université Paris Saclay, Orsay Campus, France

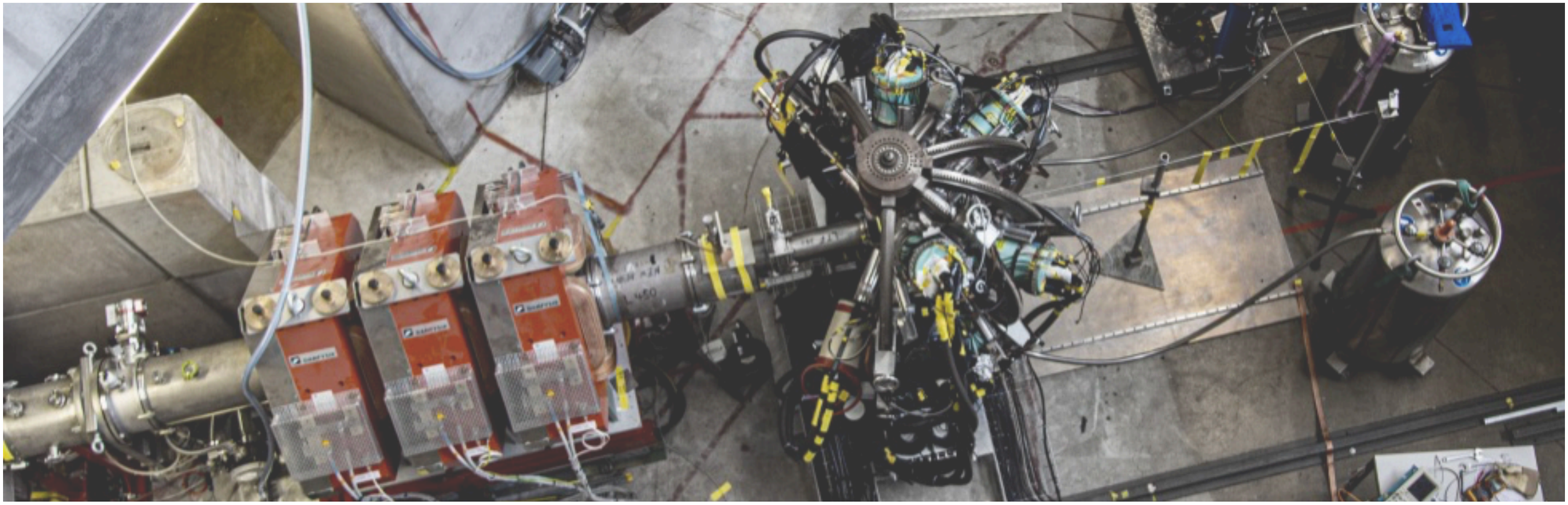

Motivation: atomic parity violation in radium

- **A**tomic **P**arity **V**iolation (APV) experiments in atoms probe the low transfer momentum Q region in the running of the $\sin^2(\theta_W)$ plot
- Weak interactions of nucleus and leptons enable APV transitions in atoms
- APV is magnified proportionally to $\gtrsim Z^3$
  ⇒ heavy atoms are good candidates
  ⇒ experimental efforts to trap / laser cool $^{226}Ra^+$

Hyperfine Interact. 199, 9 (2011)
Phys. Rev. Lett. 122, 223001 (2019)

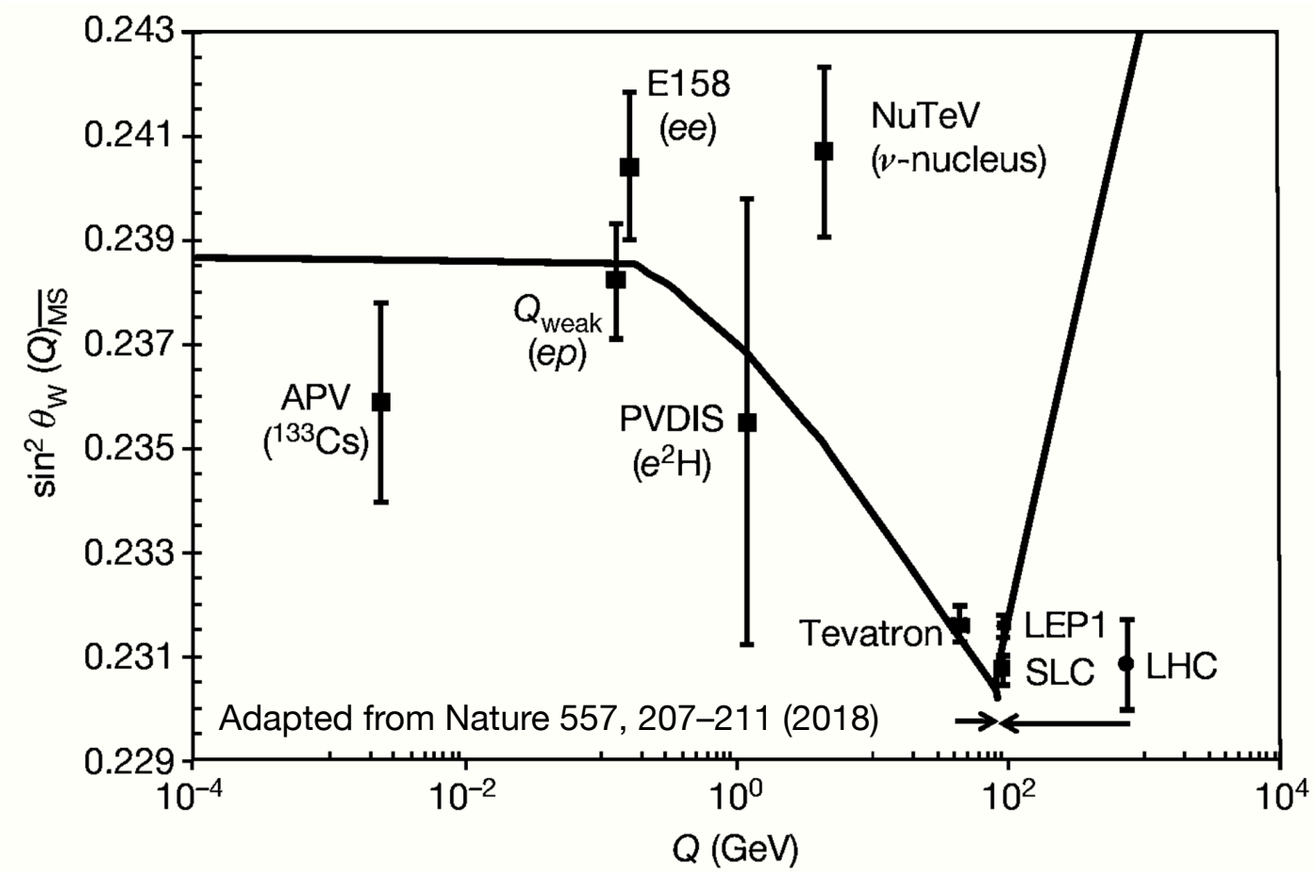

APV transitions $\propto \mathbf{k} \cdot \mathbf{Q_W}$

weak charge (related to Weinberg angle)

precision atomic calculations

The absolute nuclear charge radius of **^{226}Ra** at the level of 0.2% is needed

⇒ muX aims to measure it using muonic atoms

Motivation: atomic parity violation in radium

- **A**tomic **P**arity **V**iolation (APV) experiments in atoms probe the low transfer momentum Q region in the running of the $\sin^2(\theta_W)$ plot
- Weak interactions of nucleus and leptons enable APV transitions in atoms
- APV is magnified proportionally to $\gtrsim Z^3$
  ⇒ heavy atoms are good candidates
  ⇒ experimental efforts to trap / laser cool $^{226}Ra^+$

Hyperfine Interact. 199, 9 (2011)
Phys. Rev. Lett. 122, 223001 (2019)

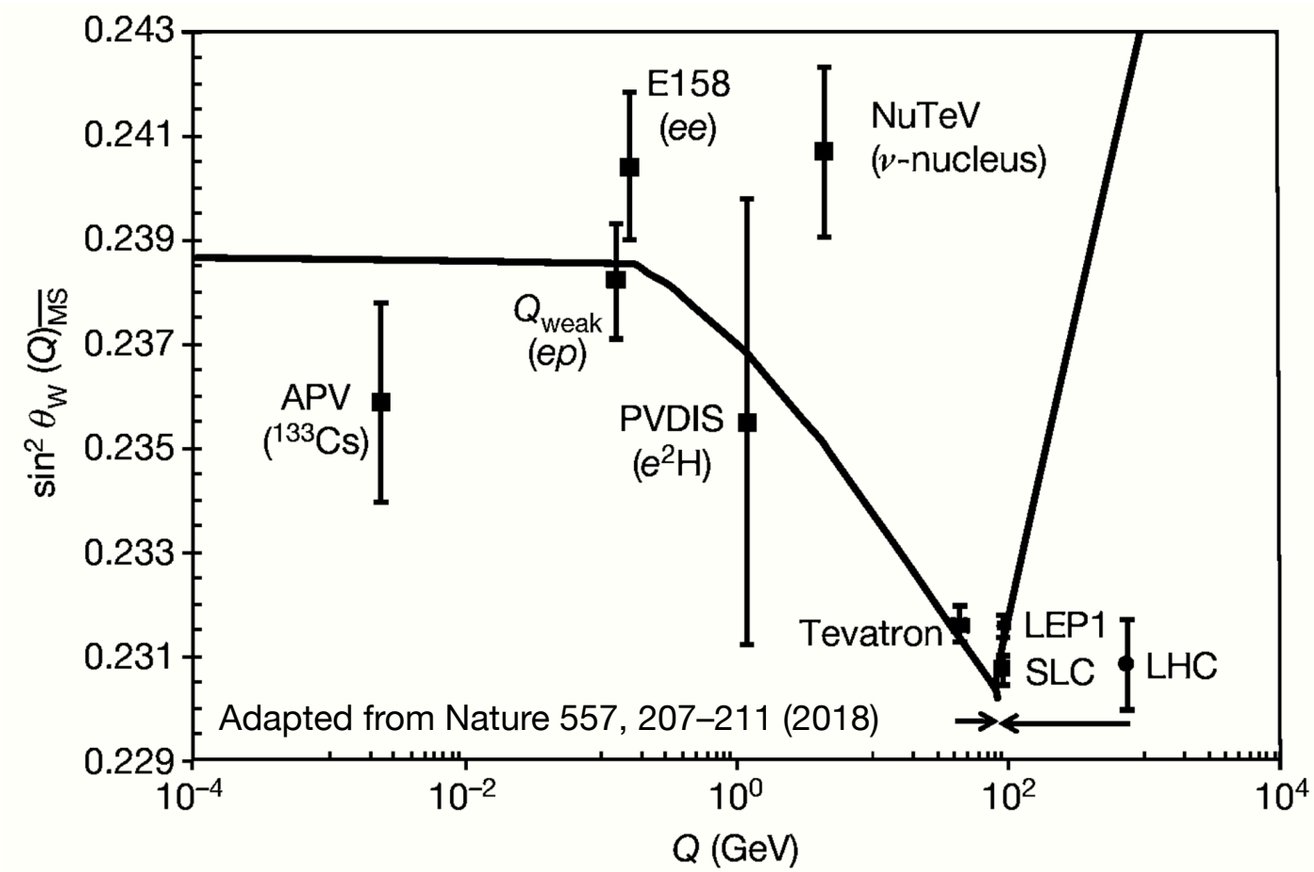

APV transitions $\propto \mathbf{k} \cdot \mathbf{Q_W}$

weak charge (related to Weinberg angle)

precision atomic calculations

The absolute nuclear charge radius of **^{226}Ra** at the level of 0.2% is needed

⇒ muX aims to measure it using muonic atoms

What about other radioactive elements?

^{248}Cm

Muonic atom spectroscopy

- Due to the higher muon mass, there is large overlap of the low-lying muonic states with the nuclear charge distribution
  ⇒ The energy of these levels is highly affected by the nuclear structure details

- The measurement of the muonic energy levels allows to extract properties of the nucleus such as the charge radius r_C:

2p-1s transition most sensitive to r_C

$$r_C^2 = \langle r^2 \rangle = \frac{1}{Ze} \int d^3\vec{r}\, \rho(\vec{r})\, r^2$$

nuclear shape?

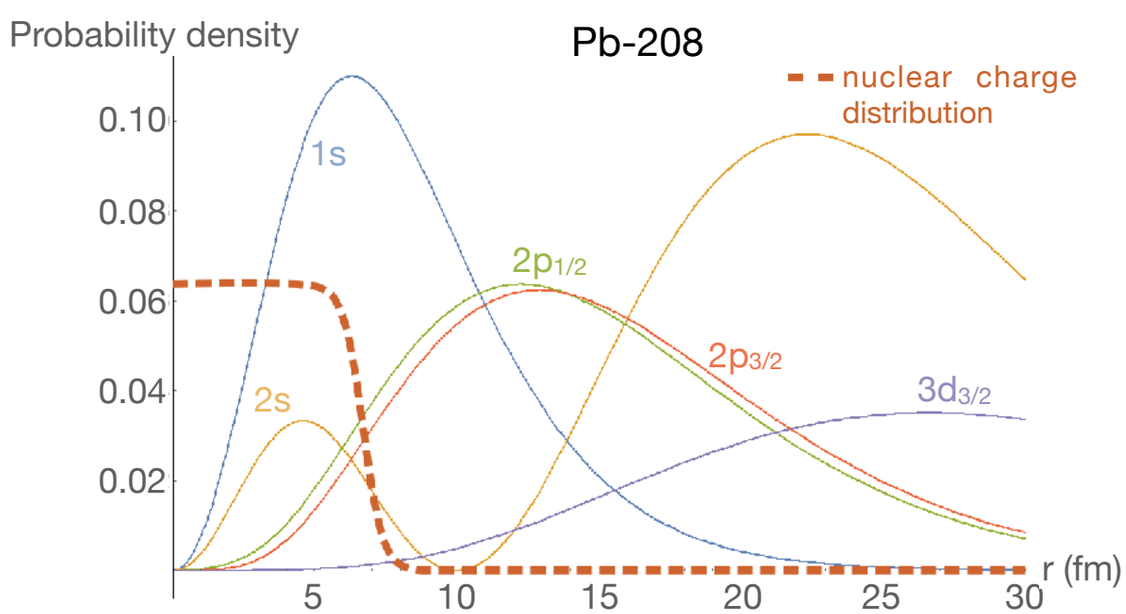

$E_{1s}(Z = 82) \sim 19\,\mathrm{MeV}$ (point nucleus)

$\sim 10.6\,\mathrm{MeV}$ (finite size)

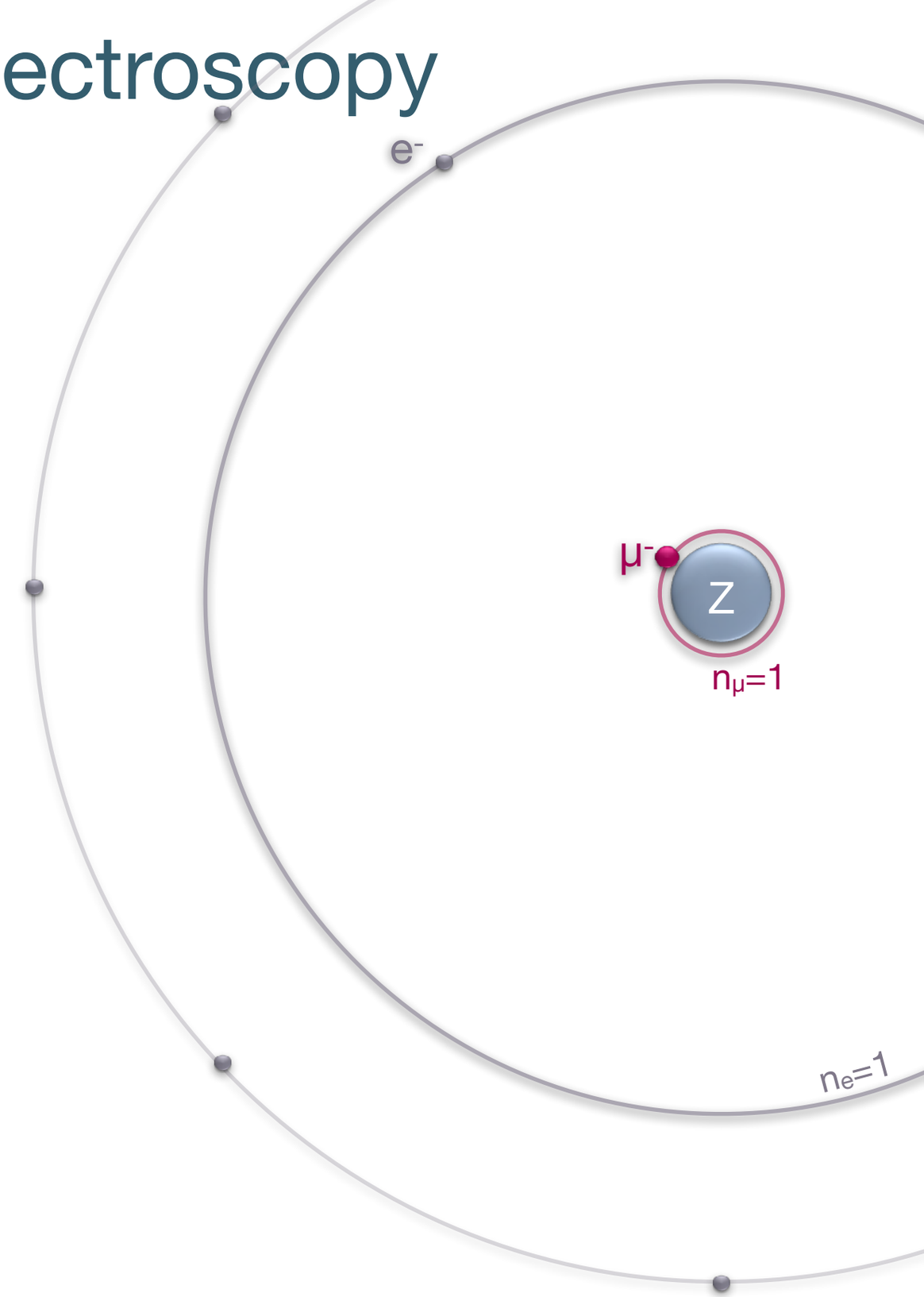

Muonic atom spectroscopy

- Due to the higher muon mass, there is large overlap of the low-lying muonic states with the nuclear charge distribution
  ⇒ The energy of these levels is highly affected by the nuclear structure details

- The measurement of the muonic energy levels allows to extract properties of the nucleus such as the charge radius r_C:

2p-1s transition most sensitive to r_C

$$r_C^2 = \langle r^2 \rangle = \frac{1}{Ze} \int d^3\vec{r}\, \rho(\vec{r})\, r^2$$

nuclear shape?

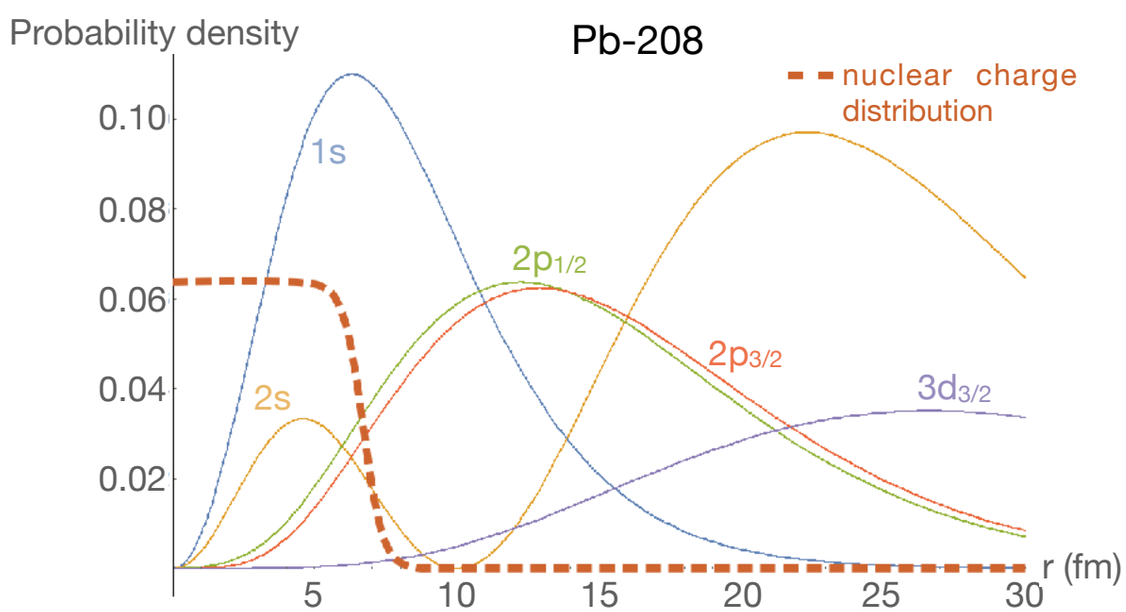

$E_{1s}(Z = 82) \sim 19\,\mathrm{MeV}$ (point nucleus)

$\sim 10.6\,\mathrm{MeV}$ (finite size)

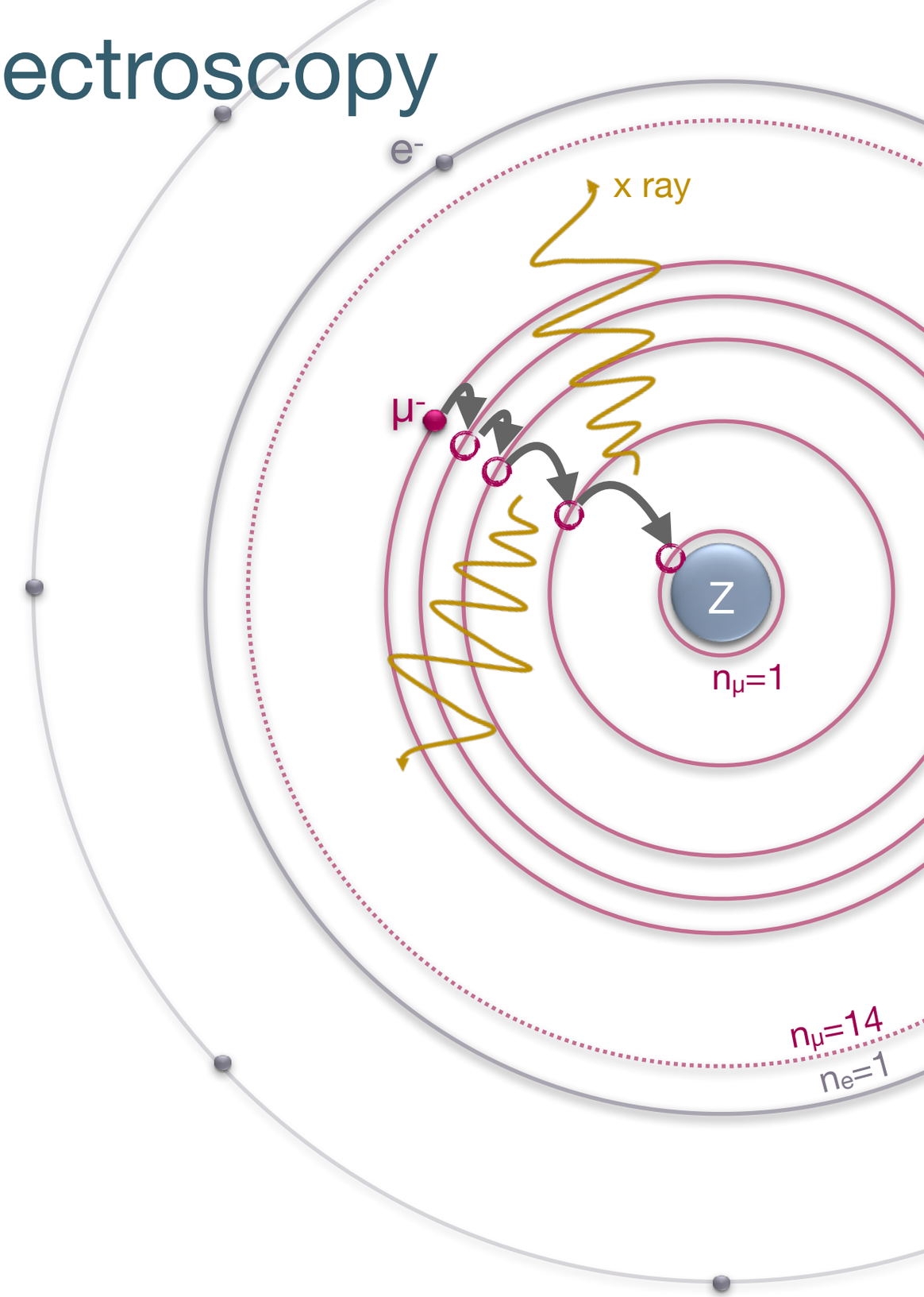

Muonic atom spectroscopy

- Due to the higher muon mass, there is large overlap of the low-lying muonic states with the nuclear charge distribution
  ⇒ The energy of these levels is highly affected by the nuclear structure details

- The measurement of the muonic energy levels allows to extract properties of the nucleus such as the charge radius r_C:

2p-1s transition most sensitive to r_C

$$r_C^2 = \langle r^2 \rangle = \frac{1}{Ze} \int d^3\vec{r}\, \rho(\vec{r})\, r^2$$

nuclear shape?

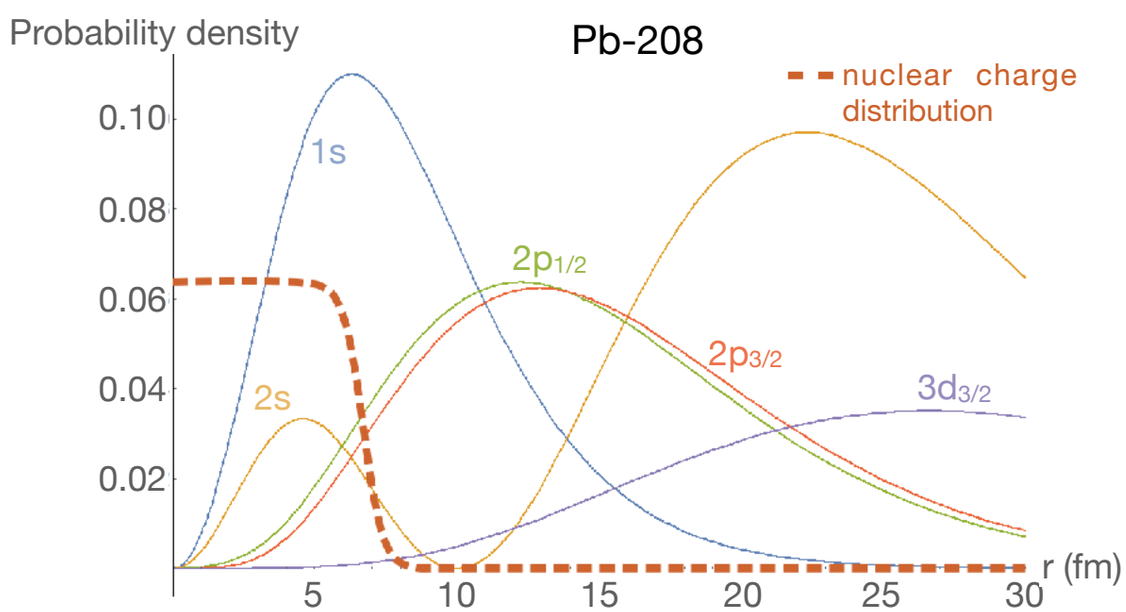

$E_{1s}(Z = 82) \sim 19\,\mathrm{MeV}$ (point nucleus)

$\sim 10.6\,\mathrm{MeV}$ (finite size)

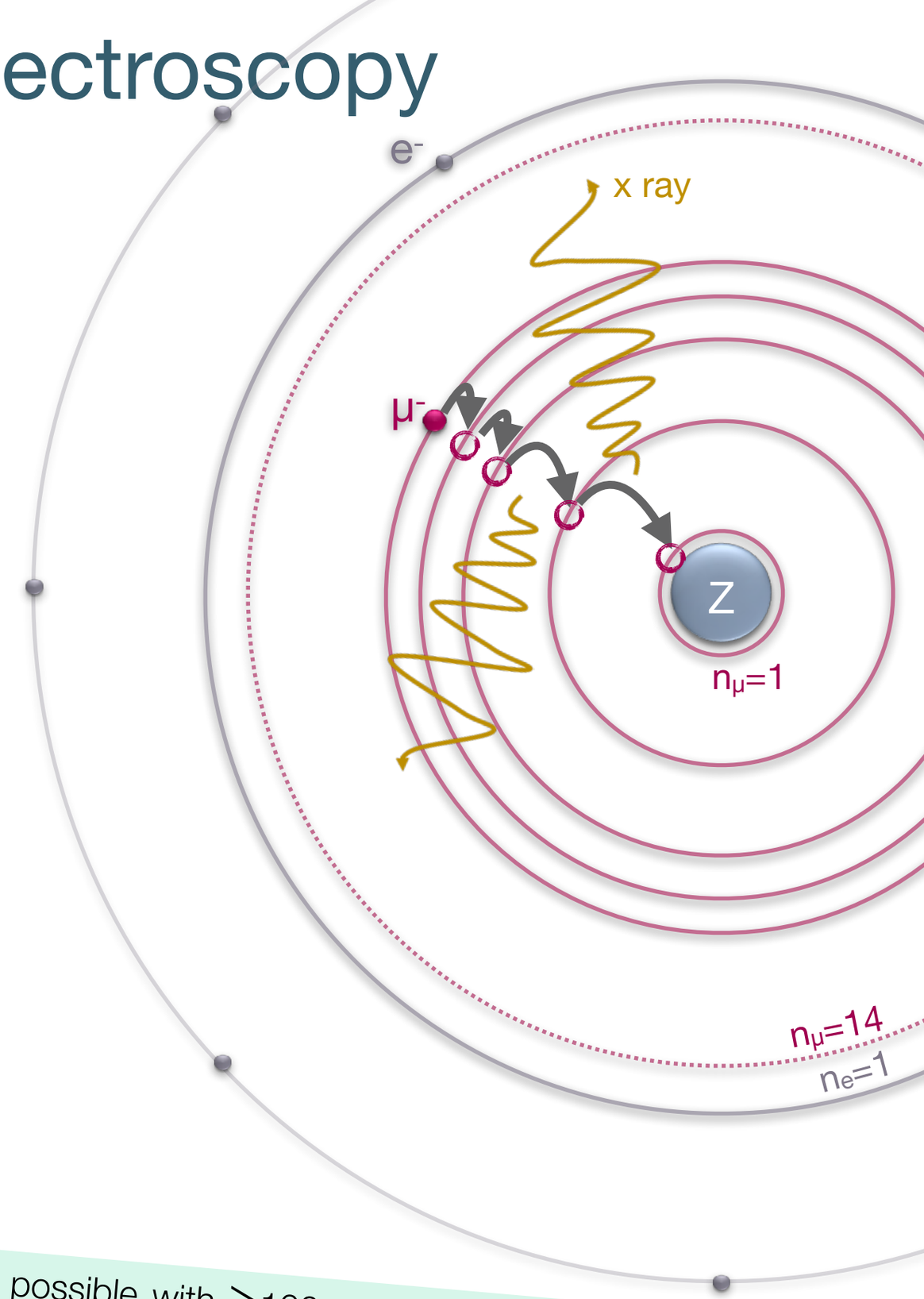

… only possible with $\gtrsim$100 mg targets… radioactive targets are typically restricted to ~μg quantities in the experimental areas

Where does this happen?

Where does this happen?

Where does this happen?

Spectroscopic quadrupole moment in ^{185,187}Re

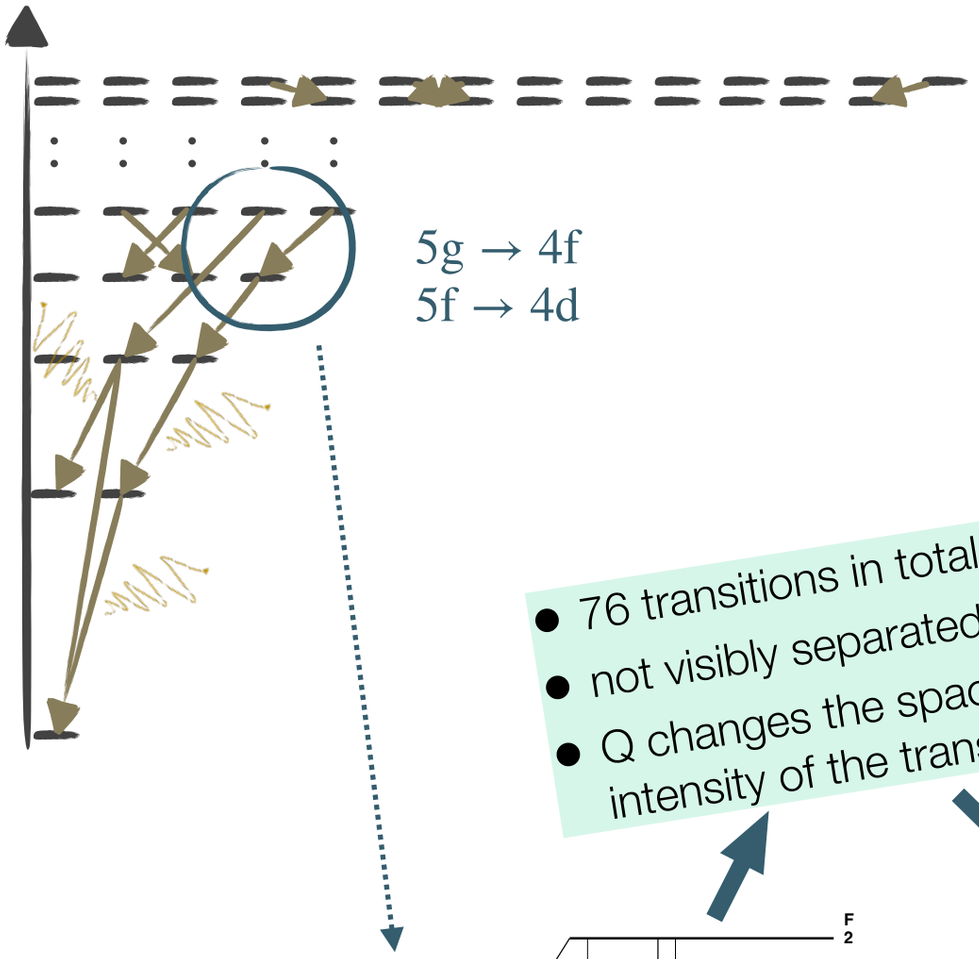

- Being sufficiently far away from the nucleus, the $5 \rightarrow 4$ transition is not sensitive to the details of the nuclear moments distribution

  ⇒ we can extract the spectroscopic quadrupole moment Q

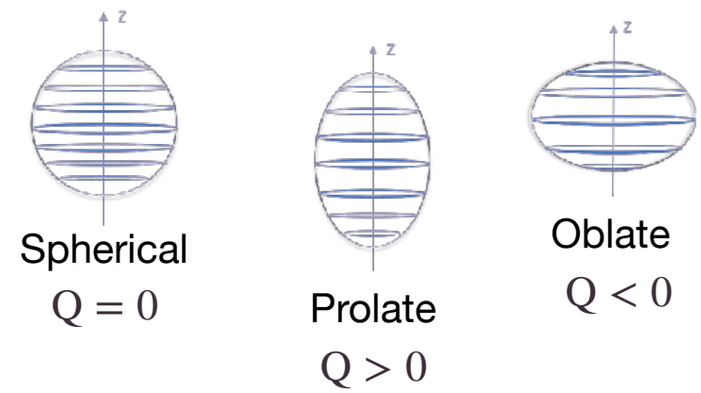

- 76 transitions in total
- not visibly separated
- Q changes the spacing and intensity of the transitions

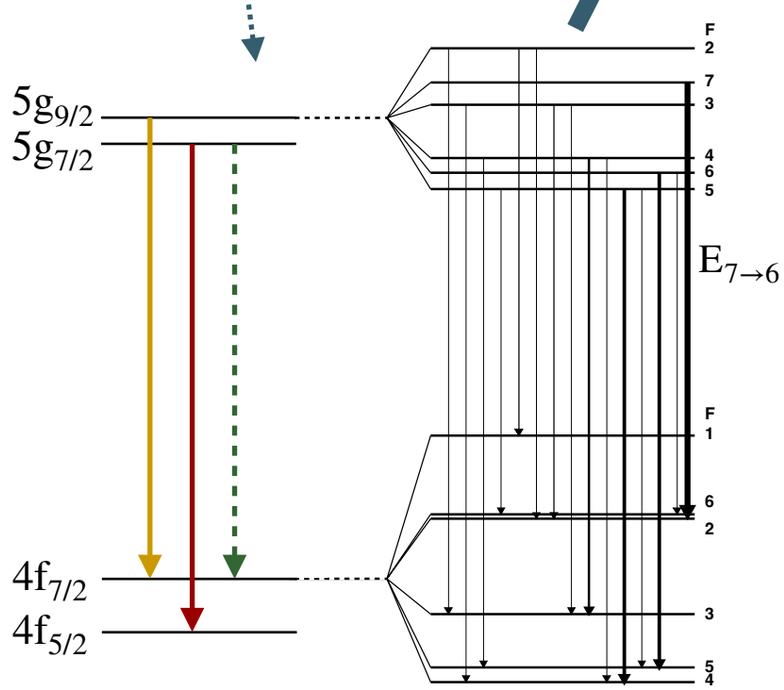

Theoretical calculations by N. Michel and N. Oreshkina, MPIK, Heidelberg

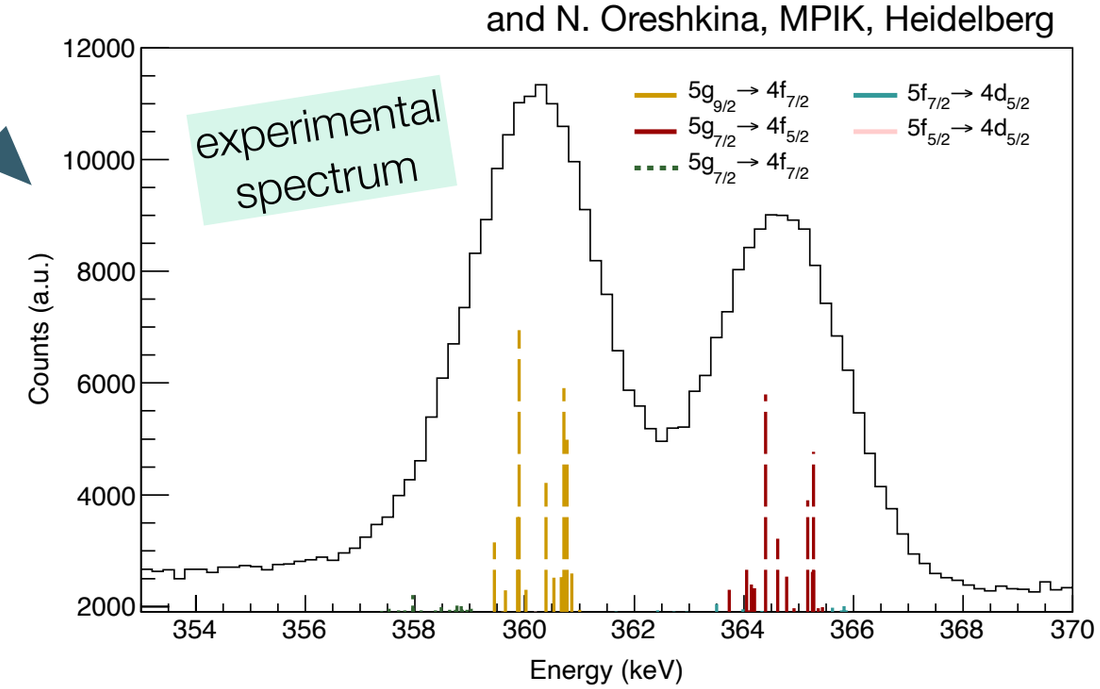

Spectroscopic quadrupole moment in ^{185,187}Re

- Fitting of the theoretical predictions in the experimental spectrum with the quadrupole moment as a free parameter
- Cross checks in two HPGe datasets

muX first physics result!
$^{185}Q = 2.07(5)$ b
$^{187}Q = 1.94(5)$ b

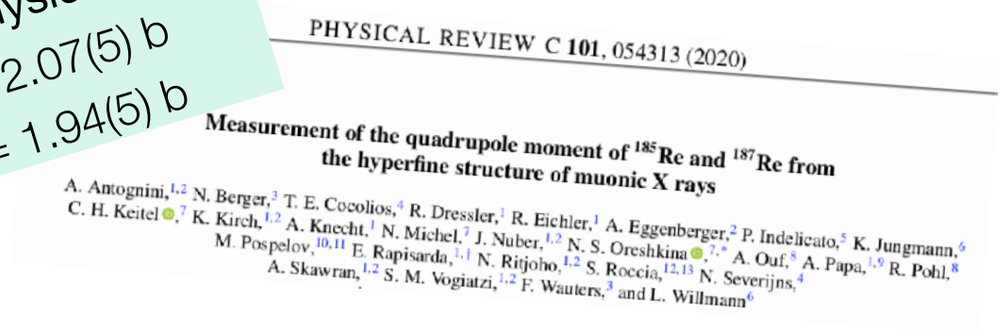
PHYSICAL REVIEW C **101**, 054313 (2020)

Measurement of the quadrupole moment of ^{185}Re and ^{187}Re from the hyperfine structure of muonic X rays

A. Antognini,[1,2] N. Berger,[3] T. E. Cocolios,[4] R. Dressler,[1] R. Eichler,[1] A. Eggenberger,[2] P. Indelicato,[5] K. Jungmann,[6] C. H. Keitel,[7] K. Kirch,[1,2] A. Knecht,[1] N. Michel,[7] J. Nuber,[1,2] N. S. Oreshkina,[7,*] A. Ouf,[8] A. Papa,[1,9] R. Pohl,[8] M. Pospelov,[10,11] E. Rapisarda,[1,1] N. Ritjoho,[1,2] S. Roccia,[12,13] N. Severijns,[4] A. Skawran,[1,2] S. M. Vogiatzi,[1,2] F. Wauters,[3] and L. Willmann[6]

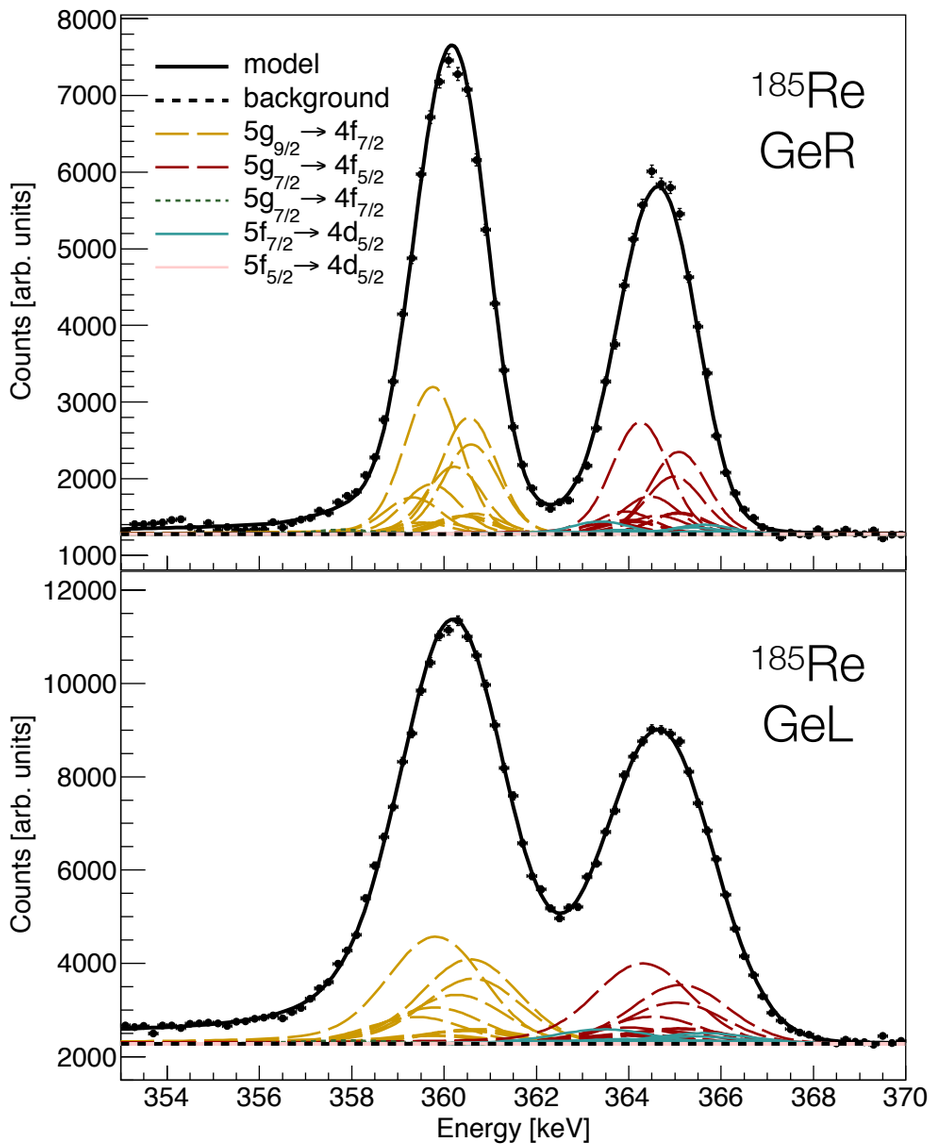

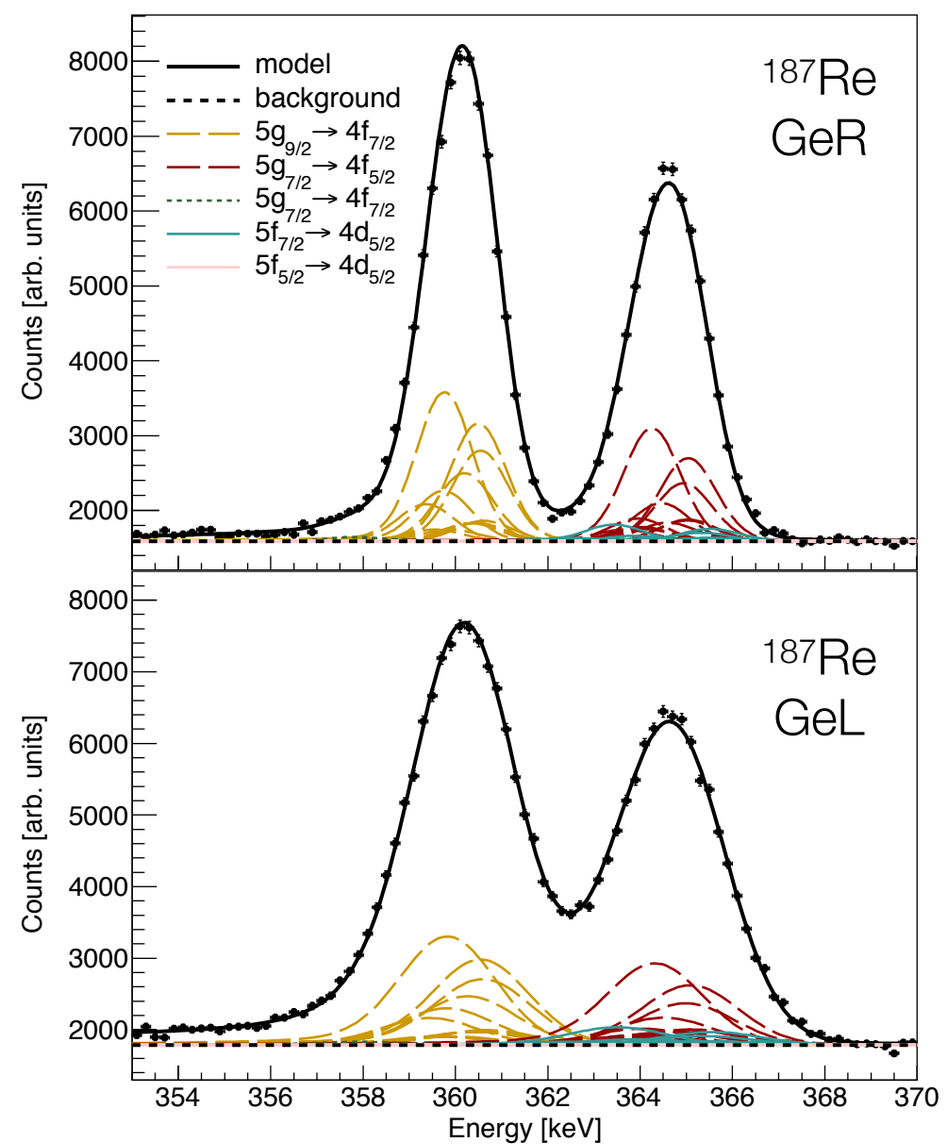

Outlook: charge radius of ^{185,187}Re

- Currently ongoing analysis of the 2p-1s hyperfine transitions in ^{185,187}Re for the extraction of its absolute nuclear charge radius
  ⇒ has not been measured before

- Complicated hyperfine structure due to the dynamic effect

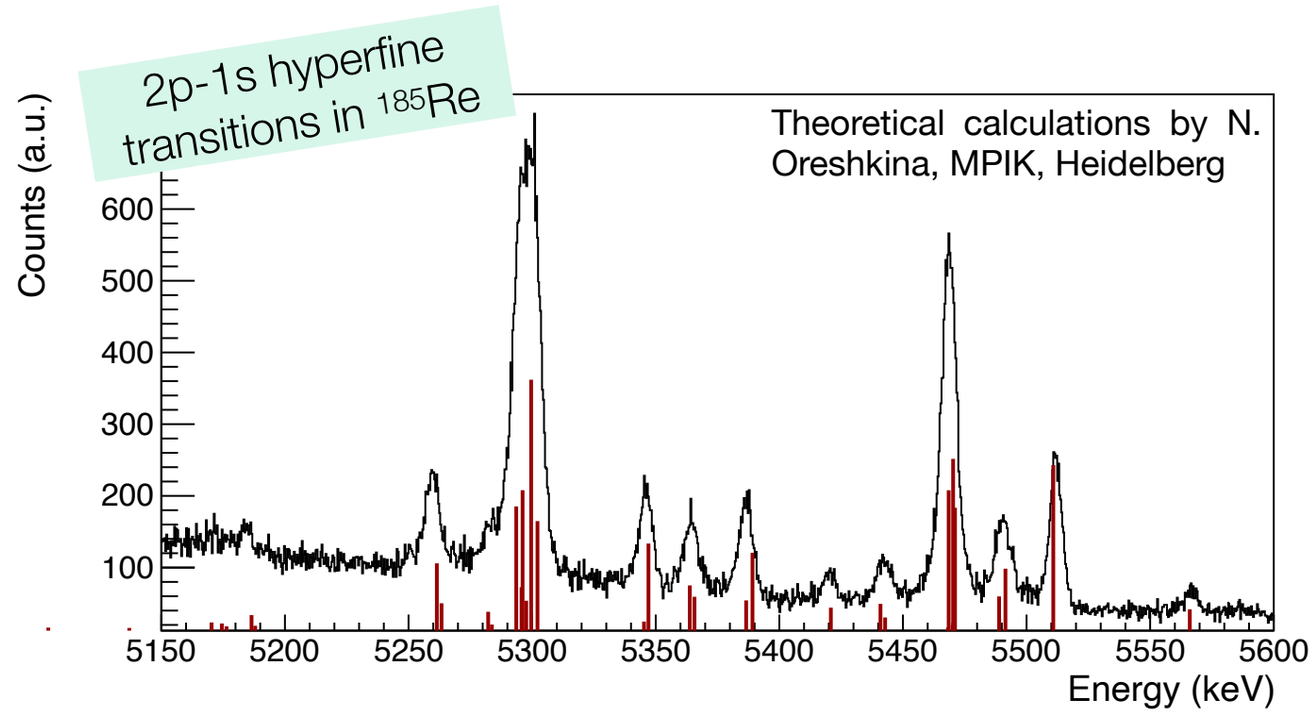

Outlook: charge radius of ^{185,187}Re

- Currently ongoing analysis of the 2p-1s hyperfine transitions in ^{185,187}Re for the extraction of its absolute nuclear charge radius
  ⇒ has not been measured before
- Complicated hyperfine structure due to the dynamic effect

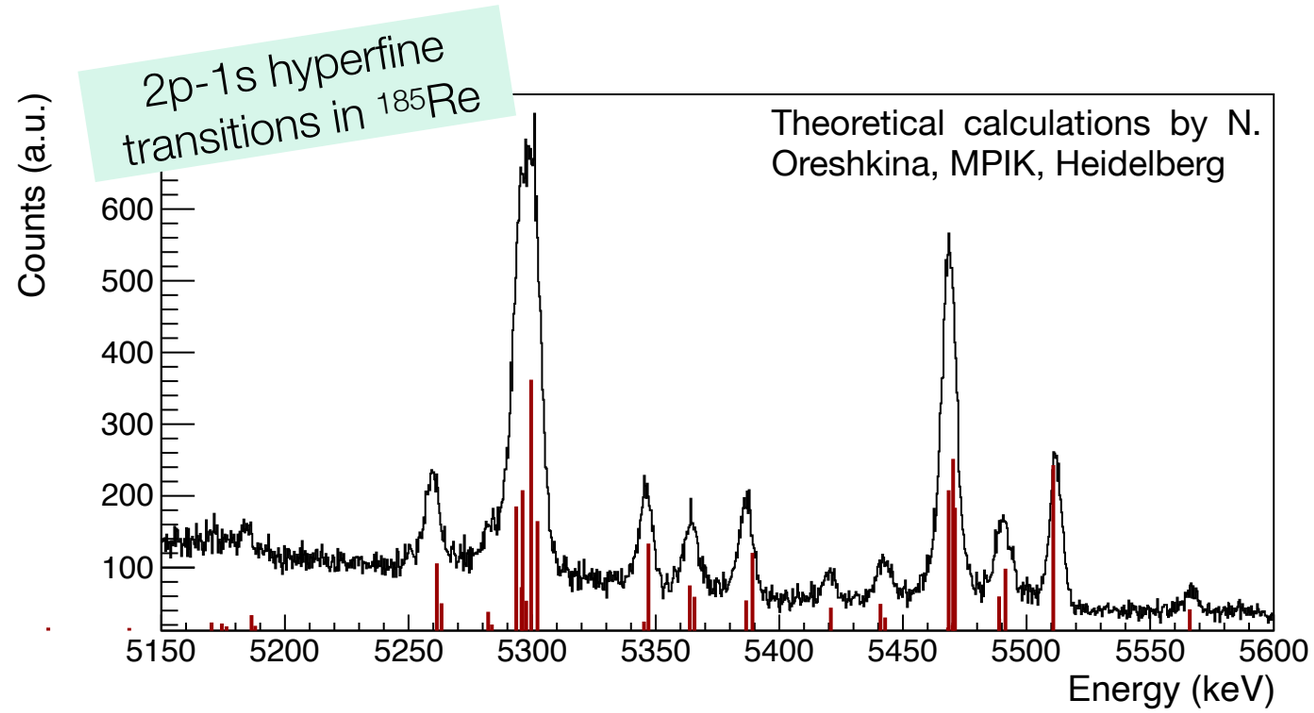

Master thesis of Jeremy Layan

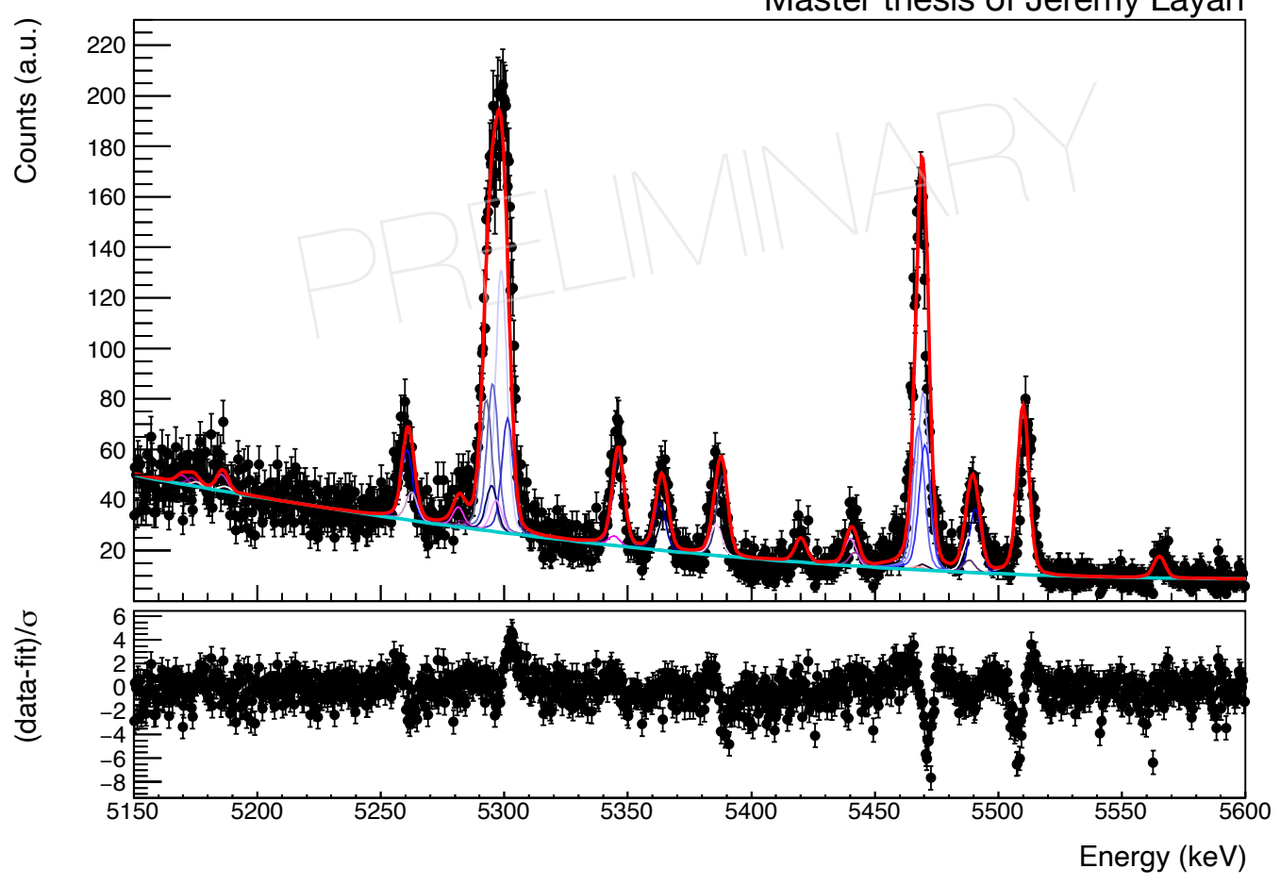

Towards the measurement of μg targets

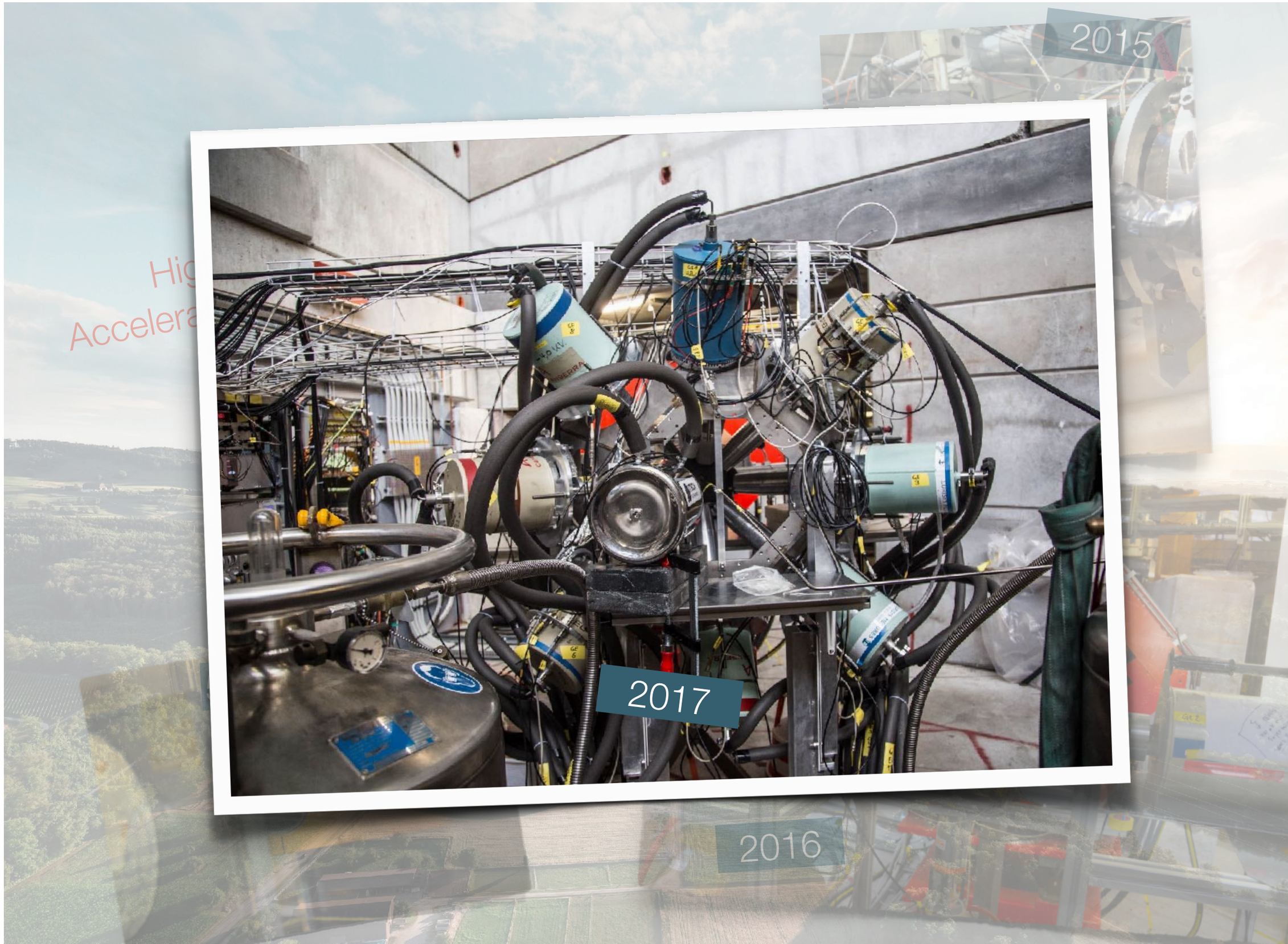

Muon transfer to microgram targets

Inspired by the work of Strasser *et al.* and Kraiman *et al.*

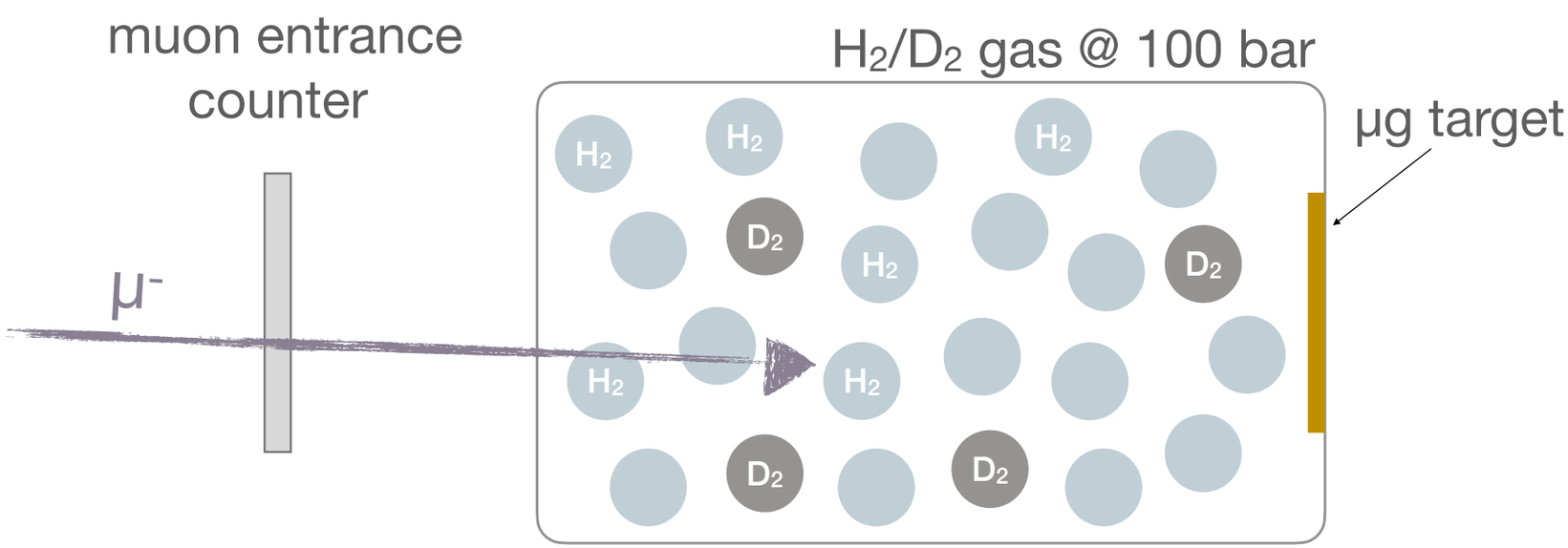

1. μ^- stops in 100 bar of H_2 + 0.1-1.5% D_2 & forms muonic hydrogen μp
2. transfer to deuterium μp → μd
3. μd moves almost freely in the H_2 gas (Ramsauer-Townsend effect[1])
4. transfer to high-Z element μd → μZ when hitting target & emission of x rays during the atomic cascade

[1] Physical Review A 73, 034501 (2006)

Muon transfer to microgram targets

Inspired by the work of Strasser *et al.* and Kraiman *et al.*

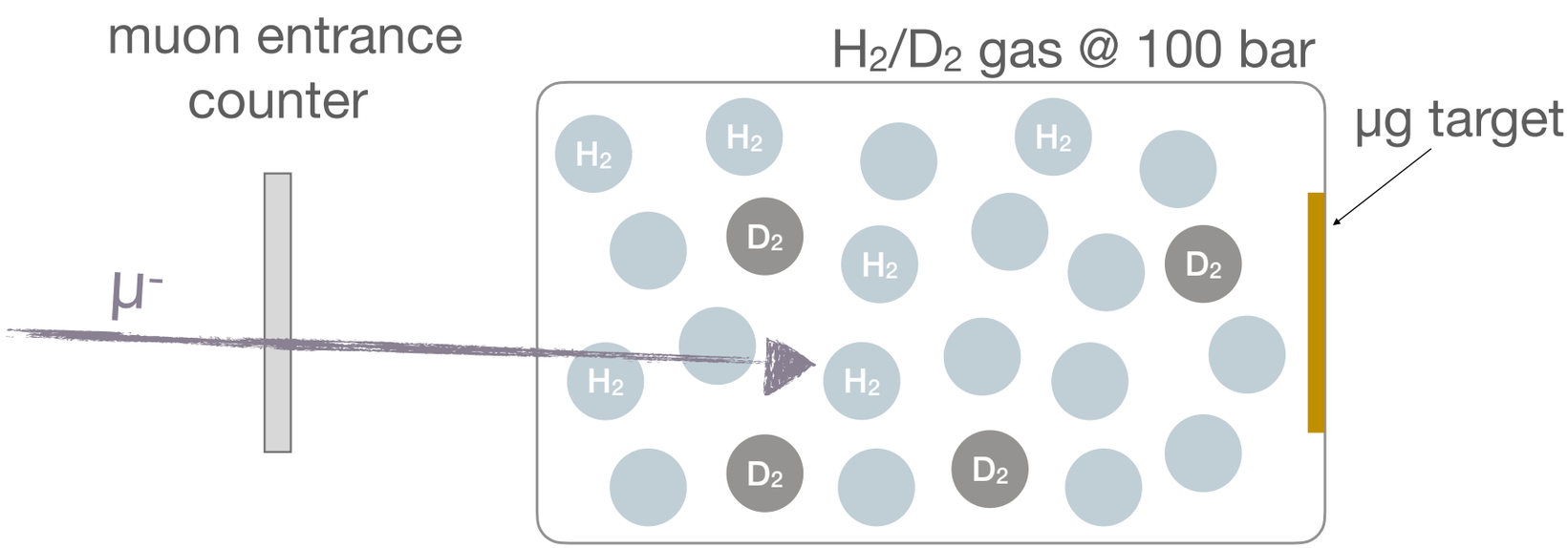

1. μ^- stops in 100 bar of H_2 + 0.1-1.5% D_2 & forms muonic hydrogen μp
2. transfer to deuterium μp → μd
3. μd moves almost freely in the H_2 gas (Ramsauer-Townsend effect[1])
4. transfer to high-Z element μd → μZ when hitting target & emission of x rays during the atomic cascade

[1] Physical Review A 73, 034501 (2006)

Muon transfer to microgram targets

Inspired by the work of Strasser *et al.* and Kraiman *et al.*

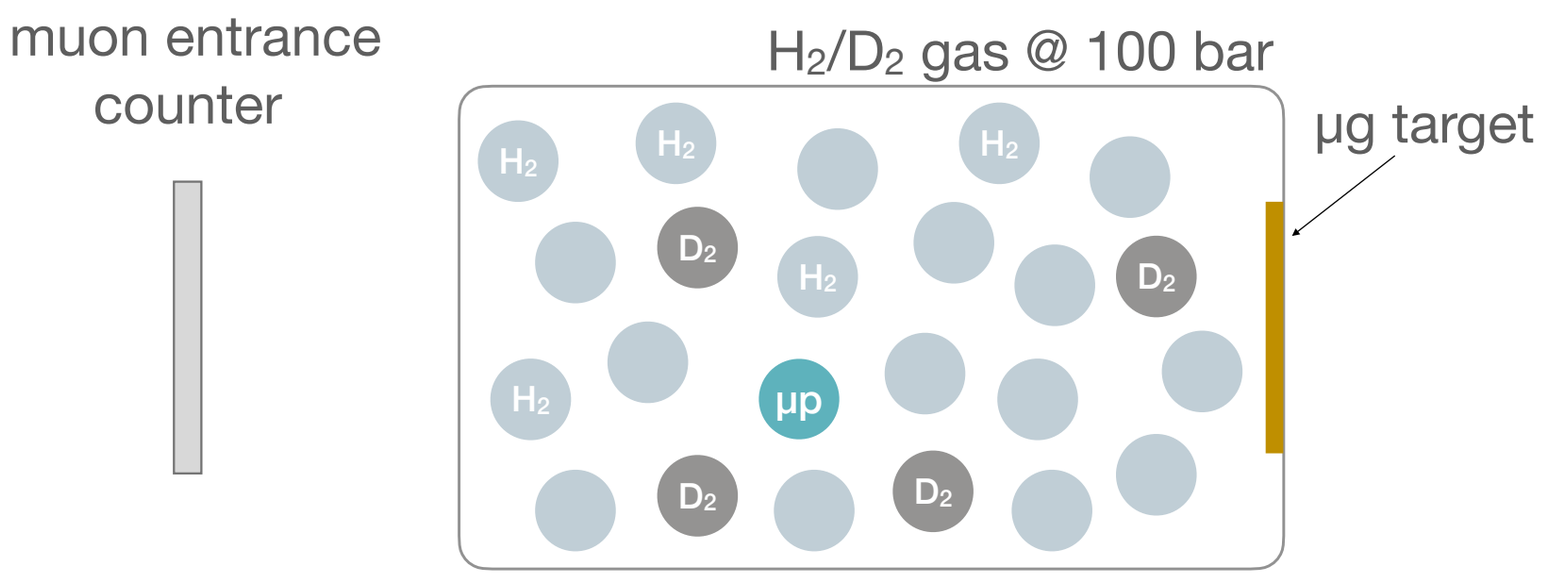

1. μ^- stops in 100 bar of H_2 + 0.1-1.5% D_2 & forms muonic hydrogen μp
2. transfer to deuterium μp → μd
3. μd moves almost freely in the H_2 gas (Ramsauer-Townsend effect[1])
4. transfer to high-Z element μd → μZ when hitting target & emission of x rays during the atomic cascade

[1] Physical Review A 73, 034501 (2006)

Muon transfer to microgram targets

Inspired by the work of Strasser *et al.* and Kraiman *et al.*

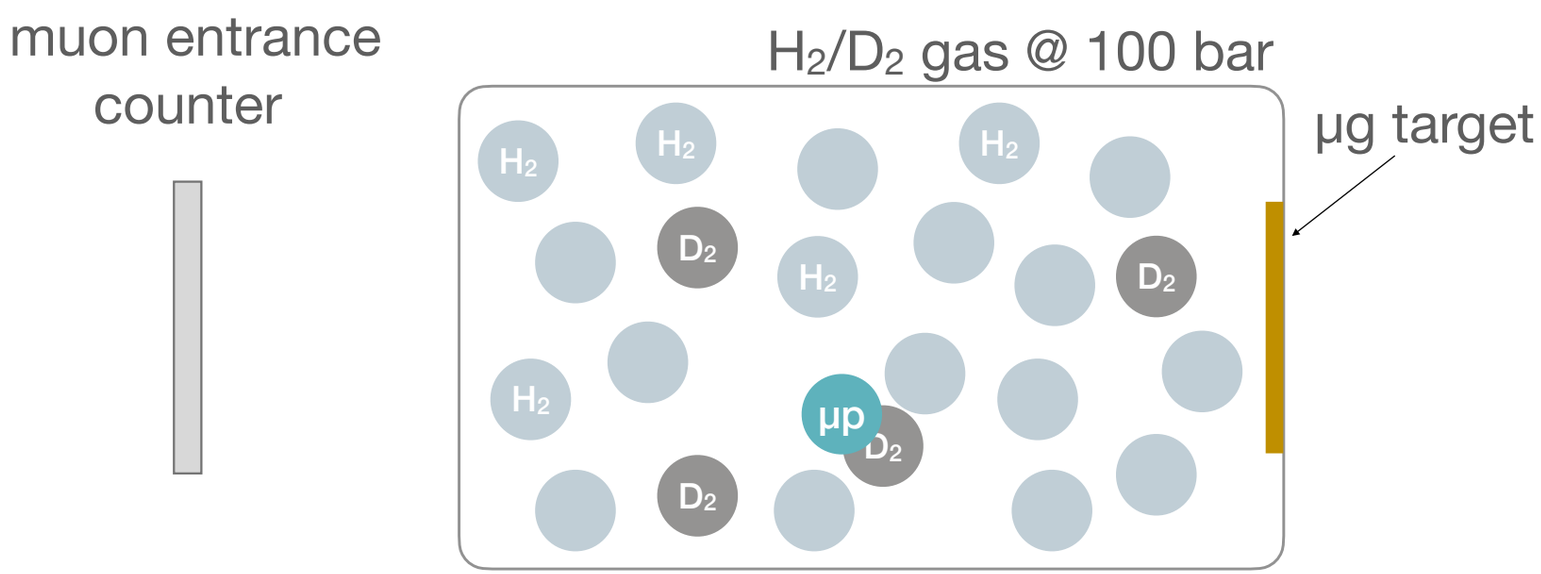

1. μ^- stops in 100 bar of H_2 + 0.1-1.5% D_2 & forms muonic hydrogen μp
2. transfer to deuterium μp → μd
3. μd moves almost freely in the H_2 gas (Ramsauer-Townsend effect[1])
4. transfer to high-Z element μd → μZ when hitting target & emission of x rays during the atomic cascade

[1] Physical Review A 73, 034501 (2006)

Muon transfer to microgram targets

Inspired by the work of Strasser *et al.* and Kraiman *et al.*

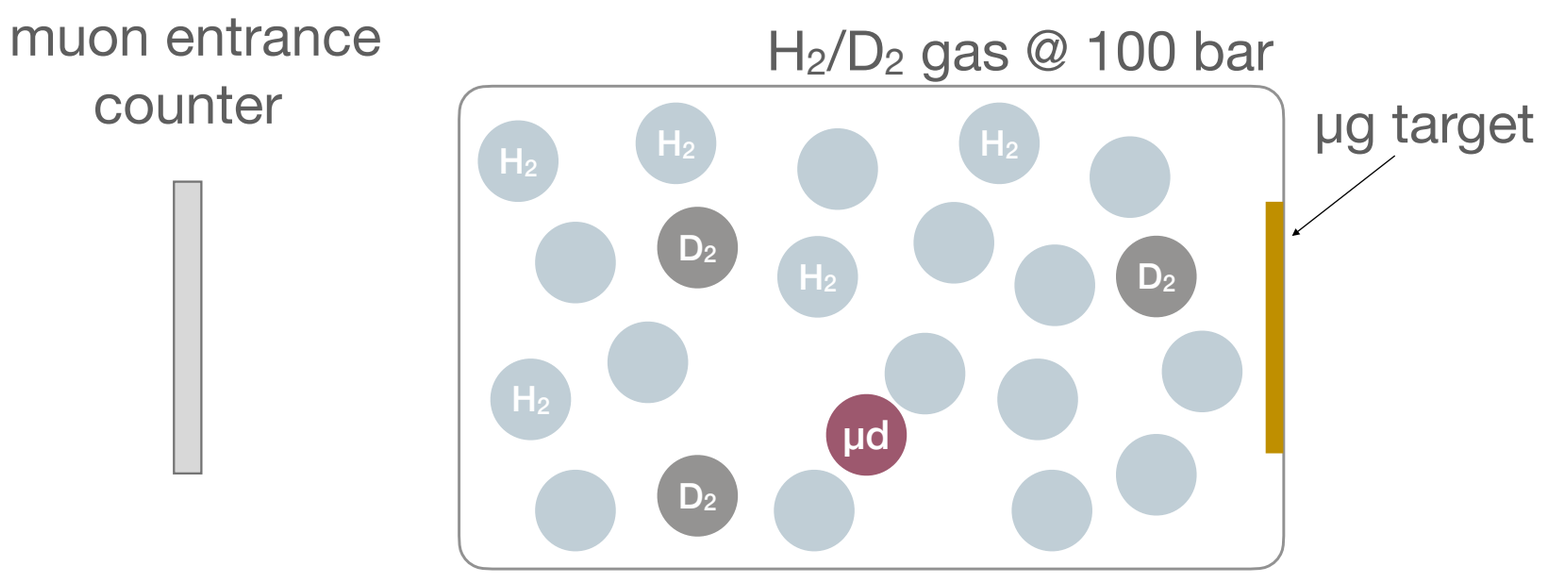

1. μ^- stops in 100 bar of H_2 + 0.1-1.5% D_2 & forms muonic hydrogen μp
2. transfer to deuterium μp → μd
3. μd moves almost freely in the H_2 gas (Ramsauer-Townsend effect[1])
4. transfer to high-Z element μd → μZ when hitting target & emission of x rays during the atomic cascade

[1] Physical Review A 73, 034501 (2006)

Muon transfer to microgram targets

Inspired by the work of Strasser *et al.* and Kraiman *et al.*

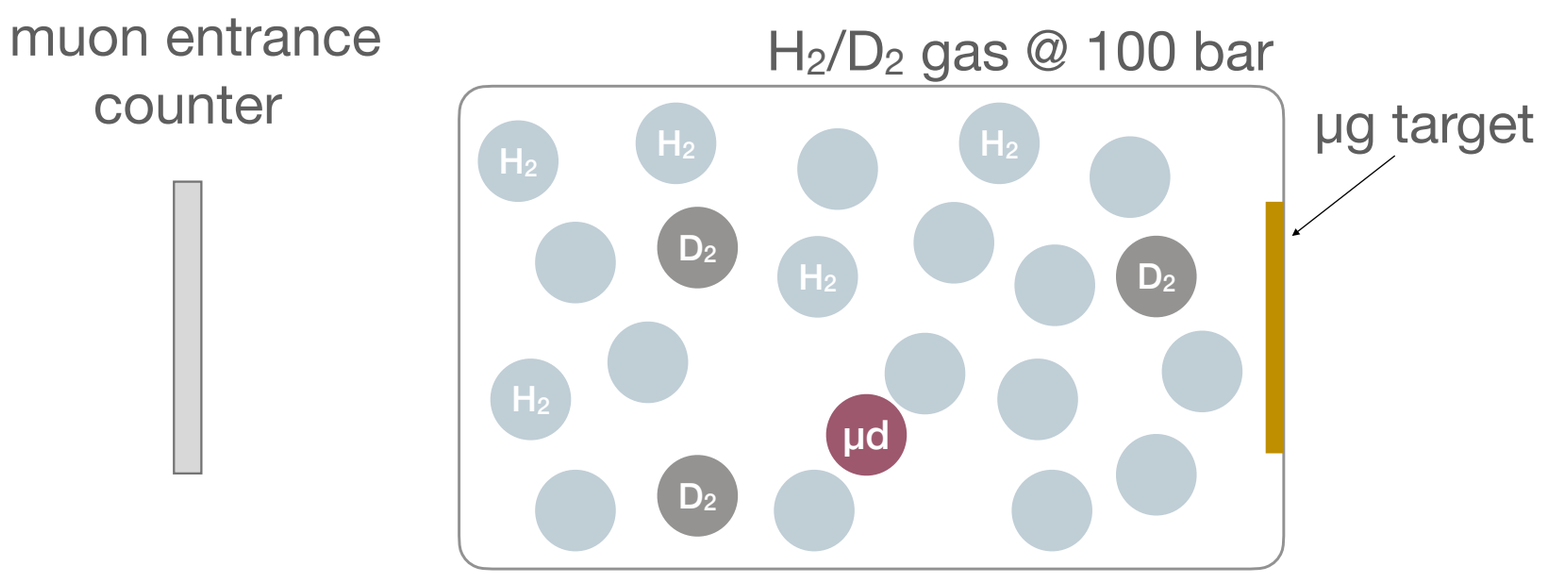

1. μ^- stops in 100 bar of H_2 + 0.1-1.5% D_2 & forms muonic hydrogen μp
2. transfer to deuterium μp → μd
3. μd moves almost freely in the H_2 gas (Ramsauer-Townsend effect[1])
4. transfer to high-Z element μd → μZ when hitting target & emission of x rays during the atomic cascade

[1] Physical Review A 73, 034501 (2006)

Muon transfer to microgram targets

Inspired by the work of Strasser *et al.* and Kraiman *et al.*

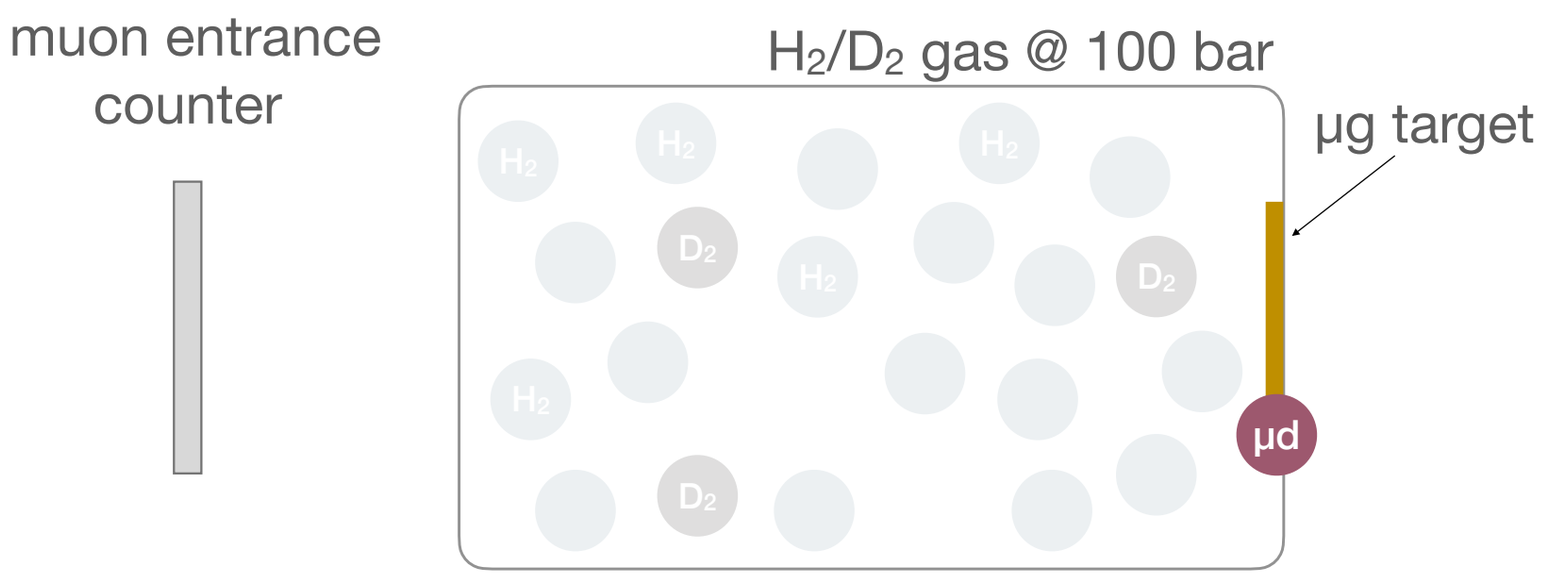

1. μ^- stops in 100 bar of H_2 + 0.1-1.5% D_2 & forms muonic hydrogen μp
2. transfer to deuterium μp → μd
3. μd moves almost freely in the H_2 gas (Ramsauer-Townsend effect[1])
4. transfer to high-Z element μd → μZ when hitting target & emission of x rays during the atomic cascade

[1] Physical Review A 73, 034501 (2006)

Muon transfer to microgram targets

Inspired by the work of Strasser *et al.* and Kraiman *et al.*

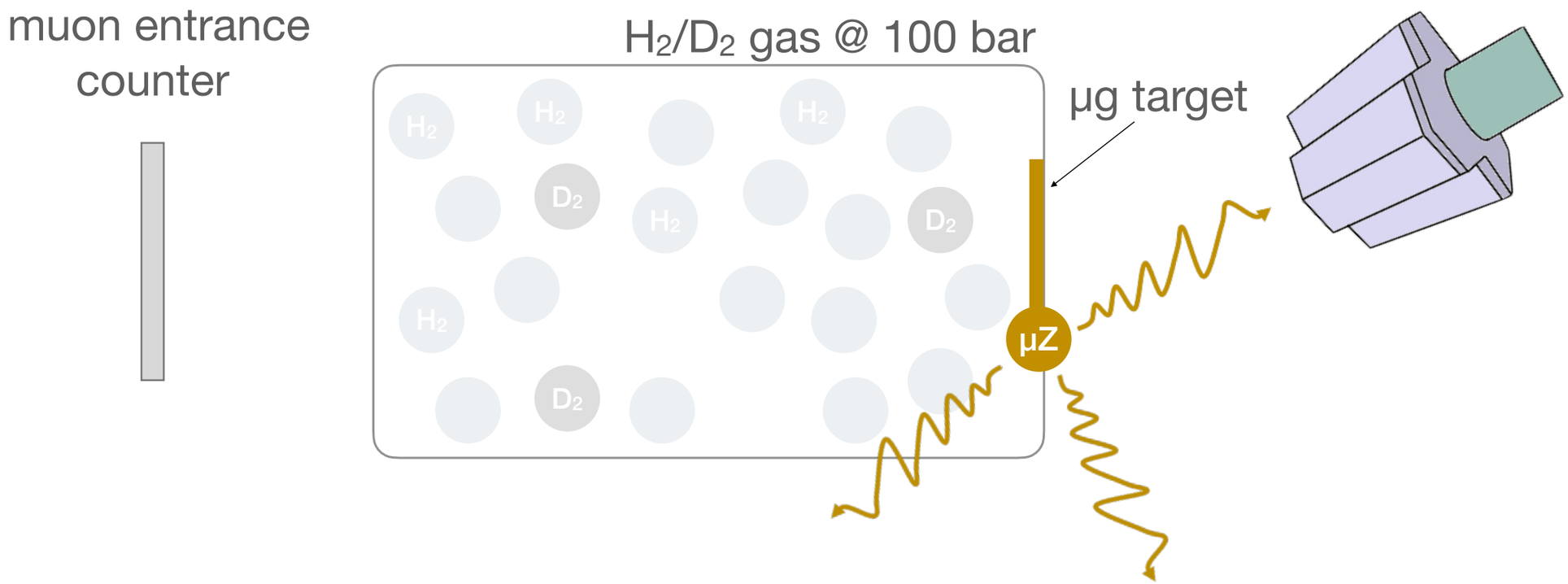

1. μ^- stops in 100 bar of H_2 + 0.1-1.5% D_2 & forms muonic hydrogen μp
2. transfer to deuterium μp → μd
3. μd moves almost freely in the H_2 gas (Ramsauer-Townsend effect[1])
4. transfer to high-Z element μd → μZ when hitting target & emission of x rays during the atomic cascade

[1] Physical Review A 73, 034501 (2006)

muX detectors

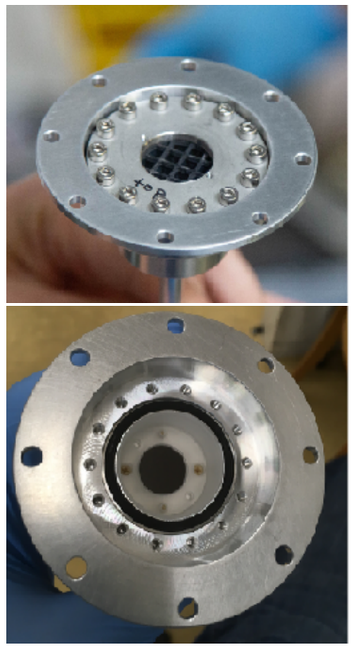

The gas cell

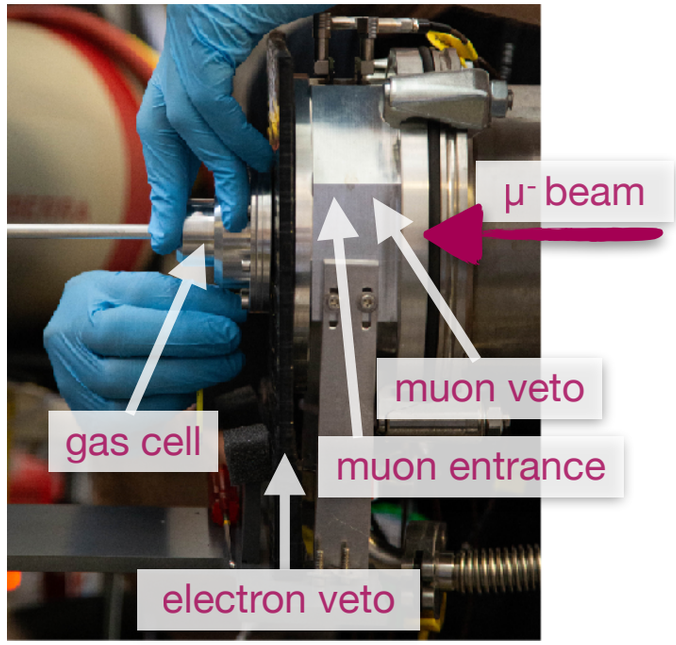

The muon and electron counters

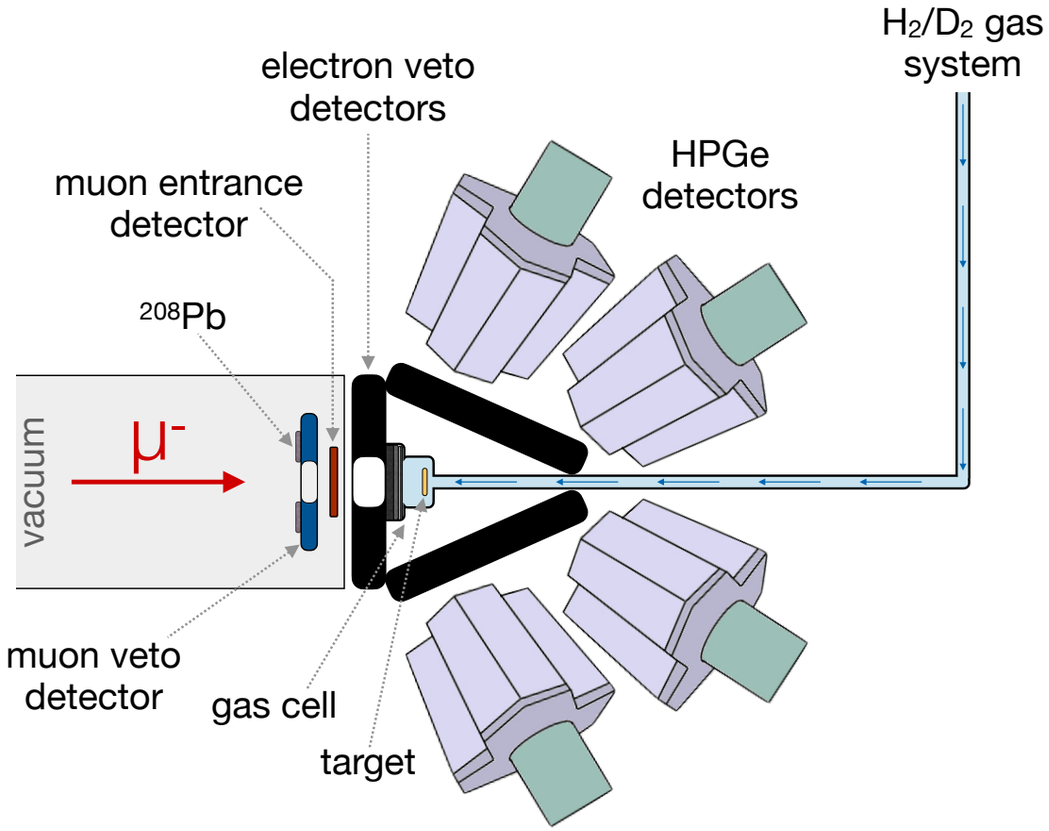

Schematics of detectors setup

muX detectors

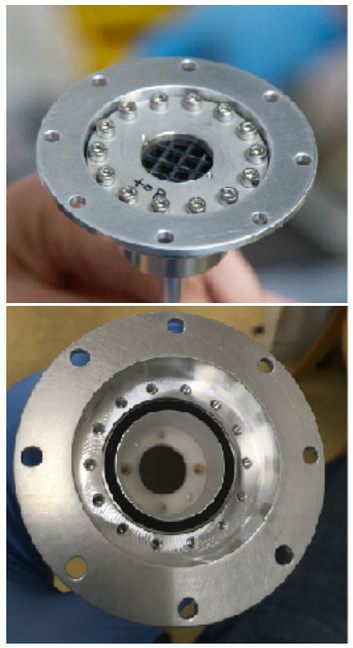

The gas cell

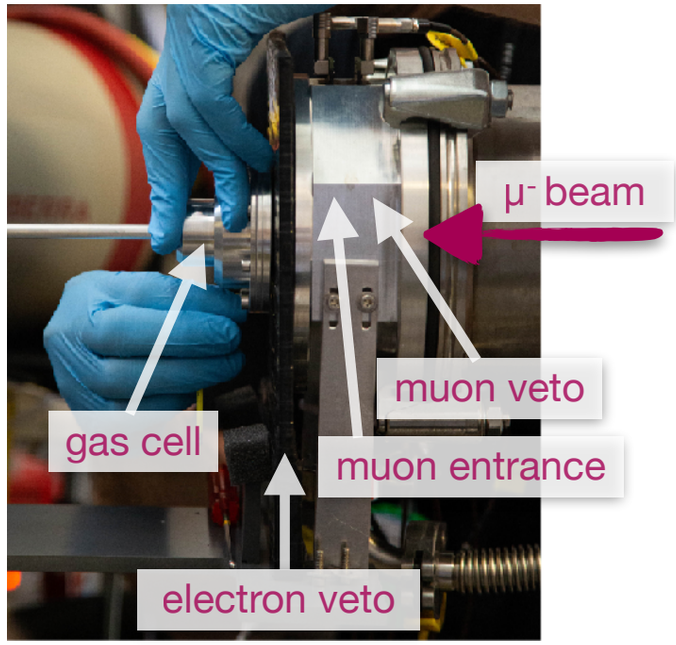

The muon and electron counters

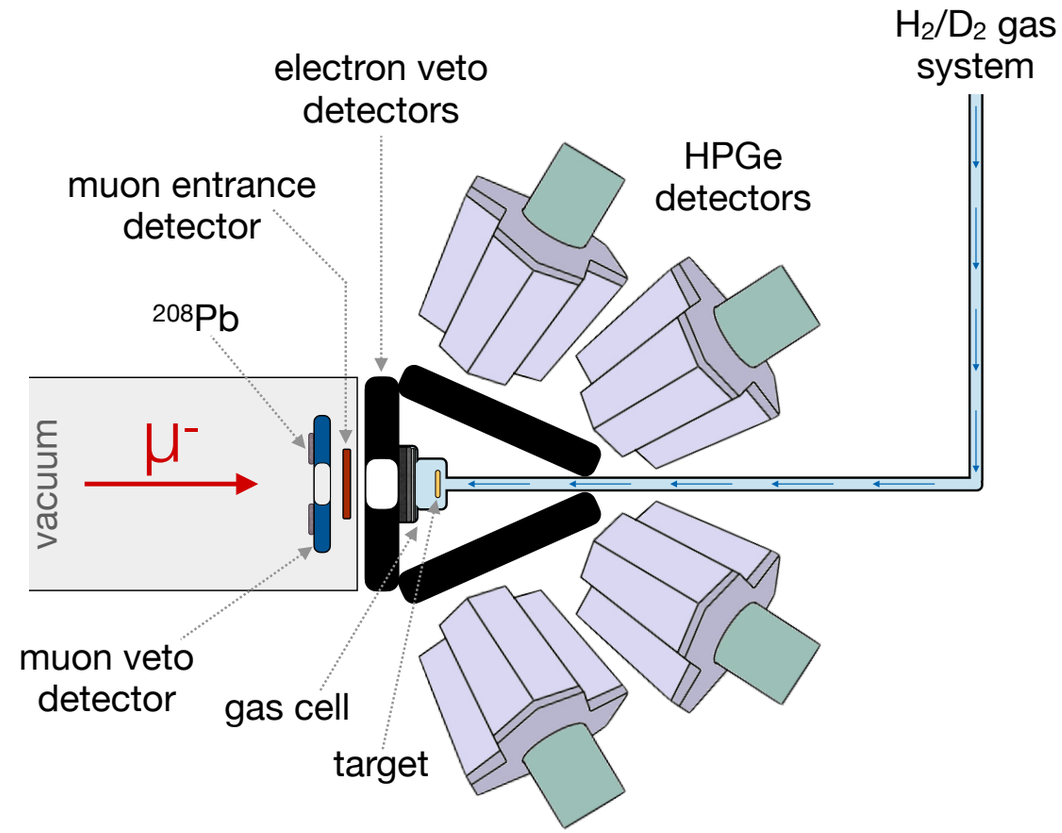

Schematics of detectors setup

Demonstration of principal in a 5 μg gold target in 2017, 18.5 h of measurement

arXiv:2209.14365

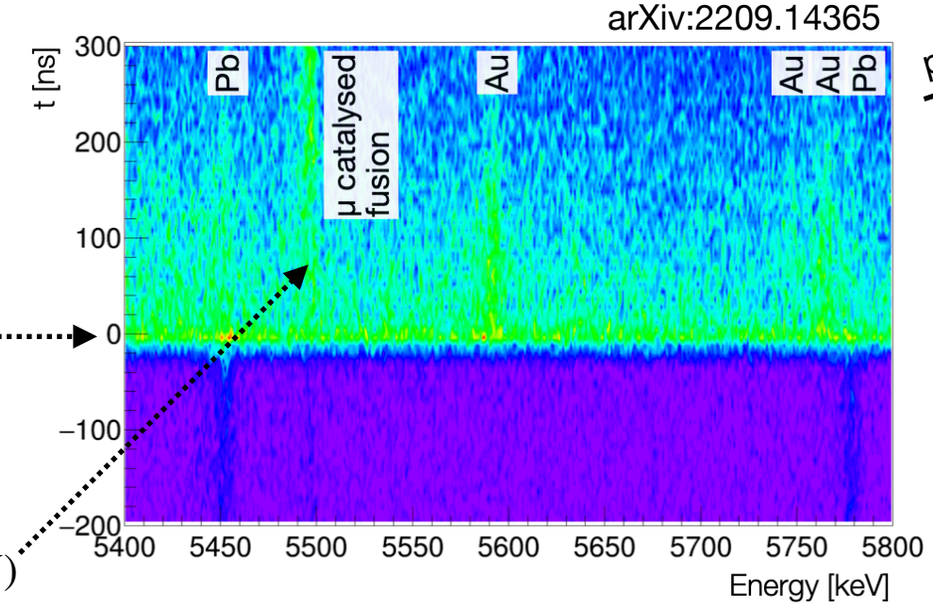

projection on energy

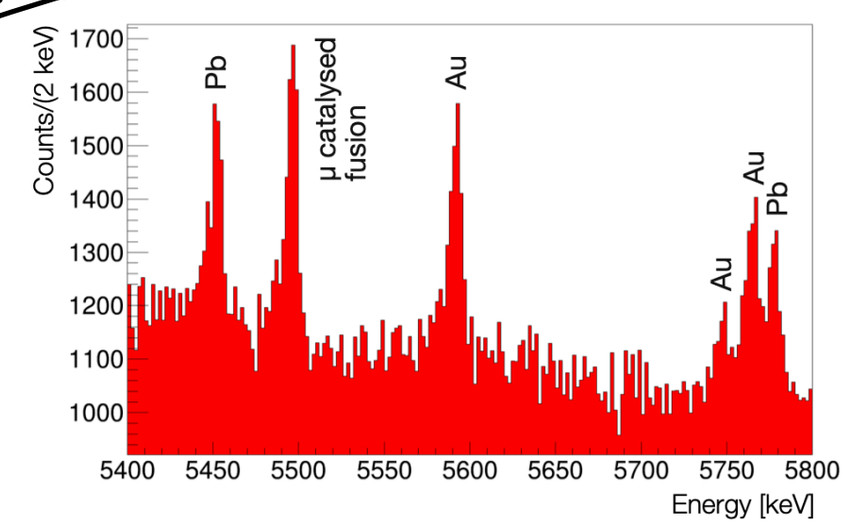

the time the muon enters the gas cell

$$\mu d + p \rightarrow p\mu d \rightarrow \mu^3He + \gamma\ (5.5\,\mathrm{MeV})$$

2019 measurement of ^{248}Cm and ^{226}Ra

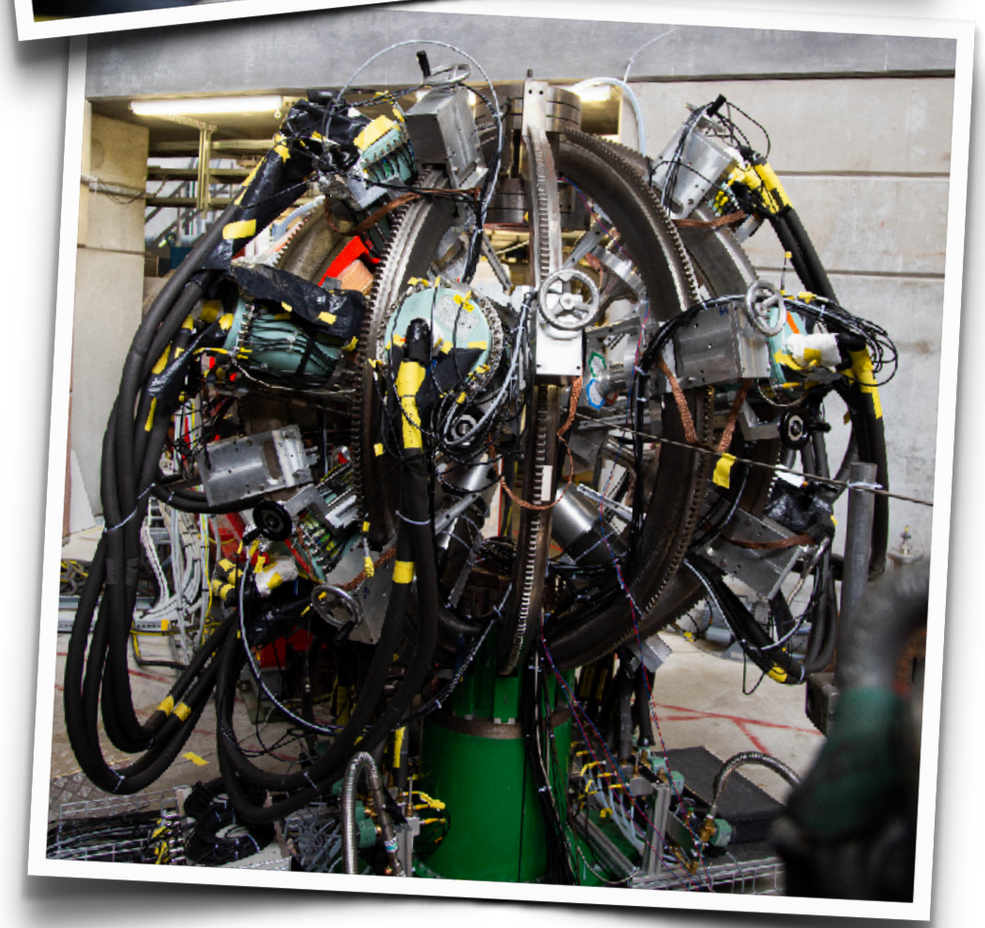

- 8 Miniball[1] germanium clusters and 2 standalone germanium detectors making a total of 26 HPGe crystals were operating [1]Eur. Phys. J. A 49, 40 (2013)
- Radiation protection restrictions at PSI allow for 16 μg of ^{248}Cm and 5.5 μg of ^{226}Ra
- Targets were produced by the radiochemistry group of the University of Mainz

^{248}Cm target

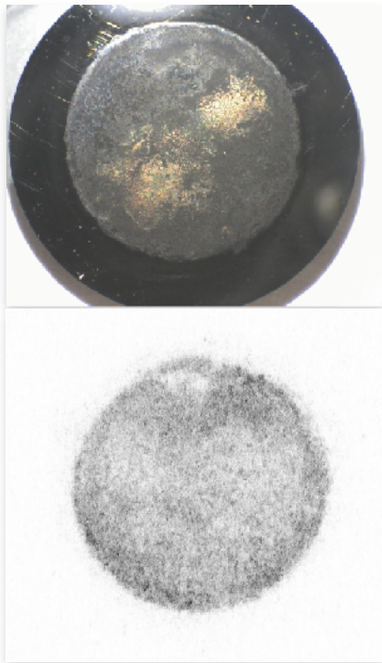

15.46 μg, uniformly distributed

^{226}Ra targets

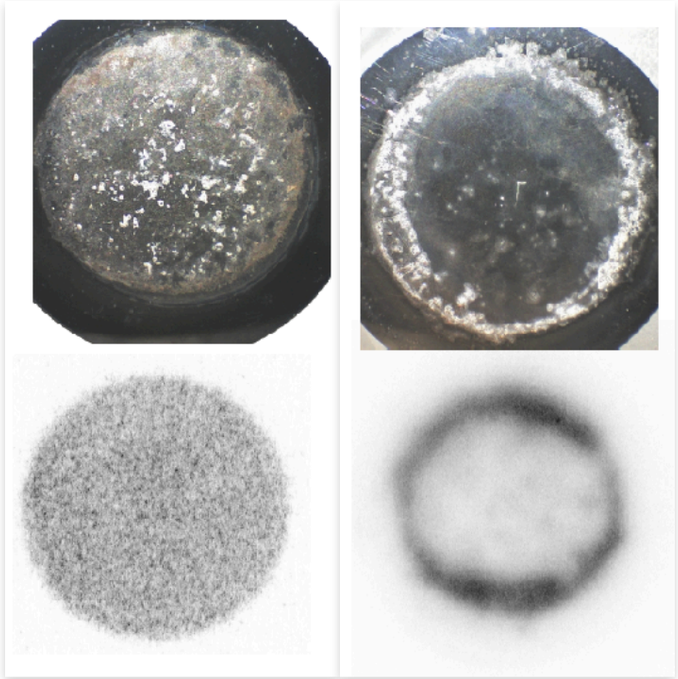

1.35 μg, uniformly distributed

4.37 μg, ring structure

2019 measurement of ^{248}Cm and ^{226}Ra

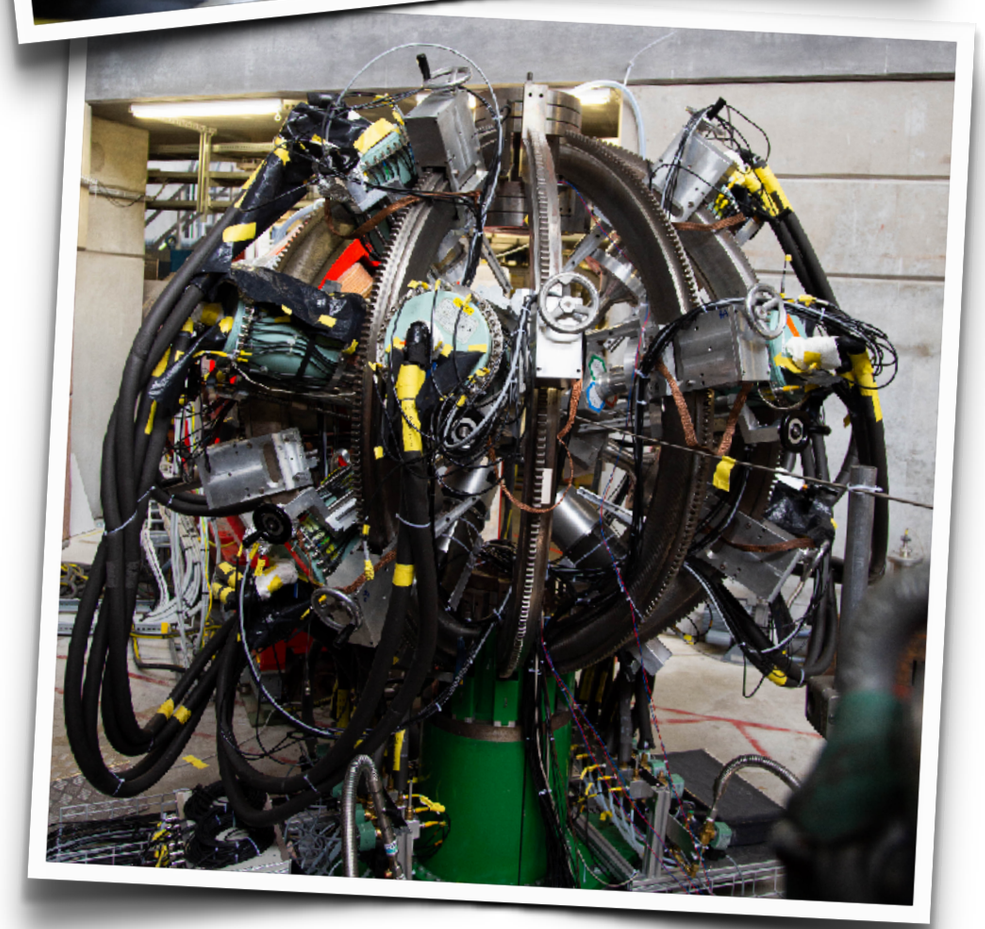

- 8 Miniball[1] germanium clusters and 2 standalone germanium detectors making a total of 26 HPGe crystals were operating [1]Eur. Phys. J. A 49, 40 (2013)
- Radiation protection restrictions at PSI allow for 16 μg of ^{248}Cm and 5.5 μg of ^{226}Ra
- Targets were produced by the radiochemistry group of the University of Mainz

^{248}Cm target

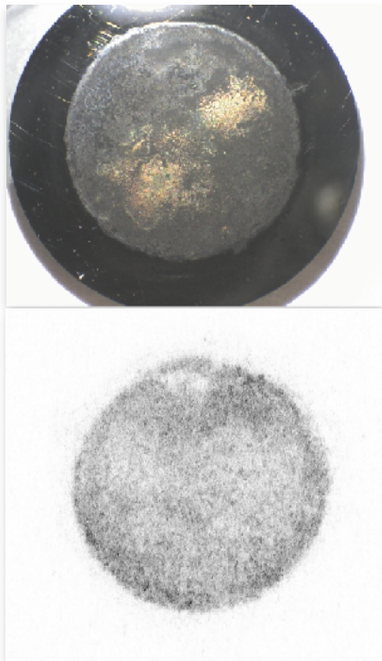

15.46 μg, uniformly distributed

^{226}Ra targets

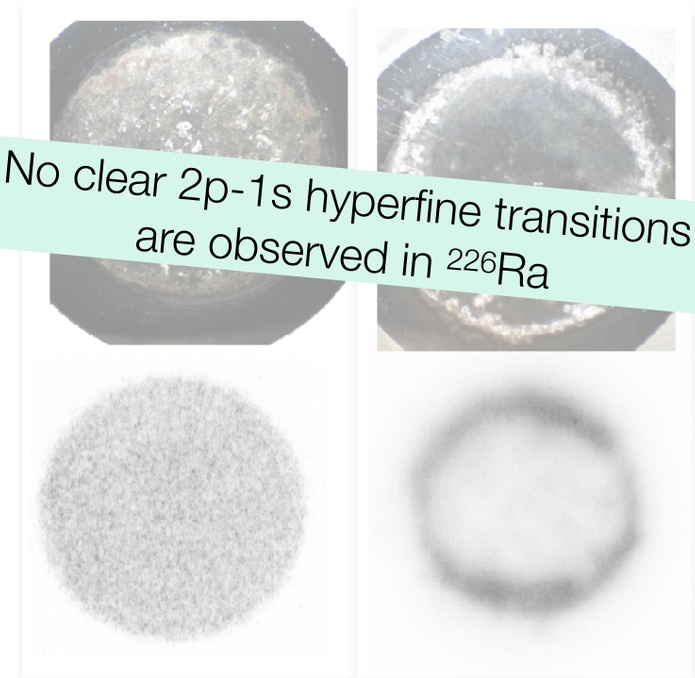

1.35 μg, uniformly distributed

4.37 μg, ring structure

No clear 2p-1s hyperfine transitions are observed in ^{226}Ra

How to get to good S/B ratio at high energies?

Cuts included:

- Electron veto anti-coincidences
- Clustering of events using the Miniball geometry
- Gain stabilisation
- Baseline correction

Most electron background is removed

$\mu^- \rightarrow e^- + \bar{\nu}_e + \nu_\mu$

Remaining neutron background

$\mu^- + (N,Z) \rightarrow (N+1,Z-1)^* + \nu_\mu$

$(N+1,Z-1)^* \rightarrow (N-x,Z-1)^* + (1+x)\,n$

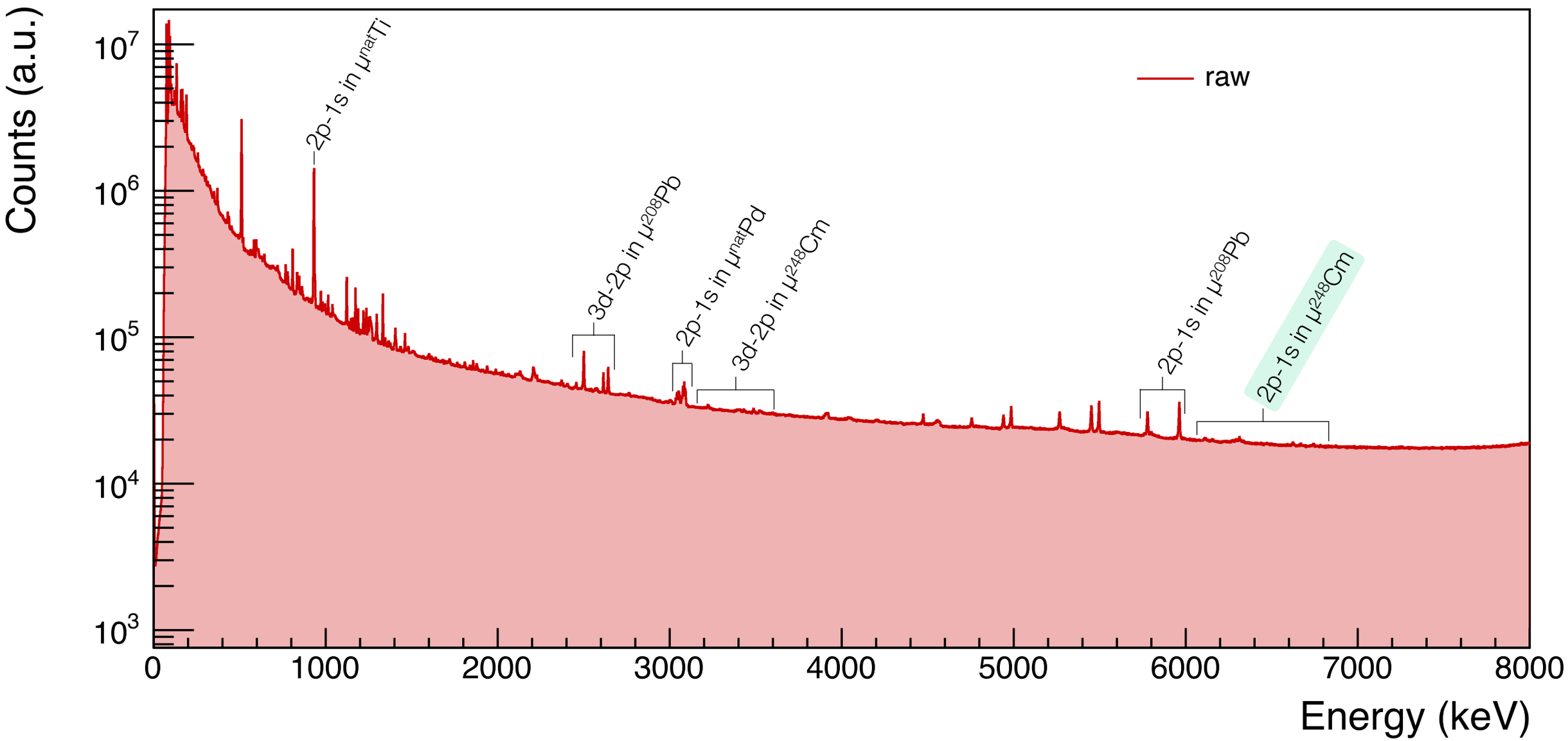

How to get to good S/B ratio at high energies?

Cuts included:

- Electron veto anti-coincidences
- Clustering of events using the Miniball geometry
- Gain stabilisation
- Baseline correction

Most electron background is removed

$\mu^- \rightarrow e^- + \bar{\nu}_e + \nu_\mu$

Remaining neutron background

$\mu^- + (N,Z) \rightarrow (N+1,Z-1)^* + \nu_\mu$

$(N+1,Z-1)^* \rightarrow (N-x,Z-1)^* + (1+x)\,n$

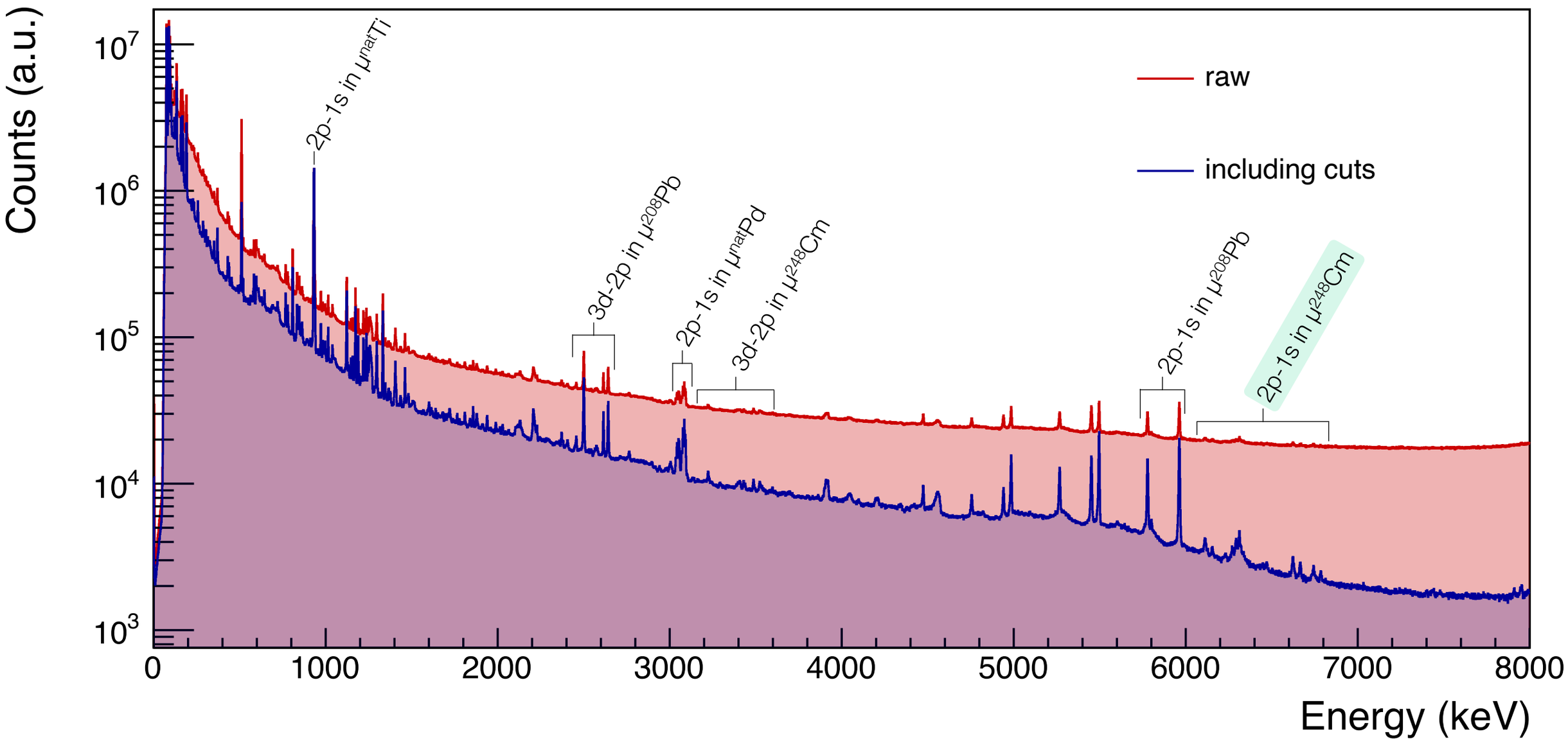

2p→1s hyperfine transitions in ^{248}Cm

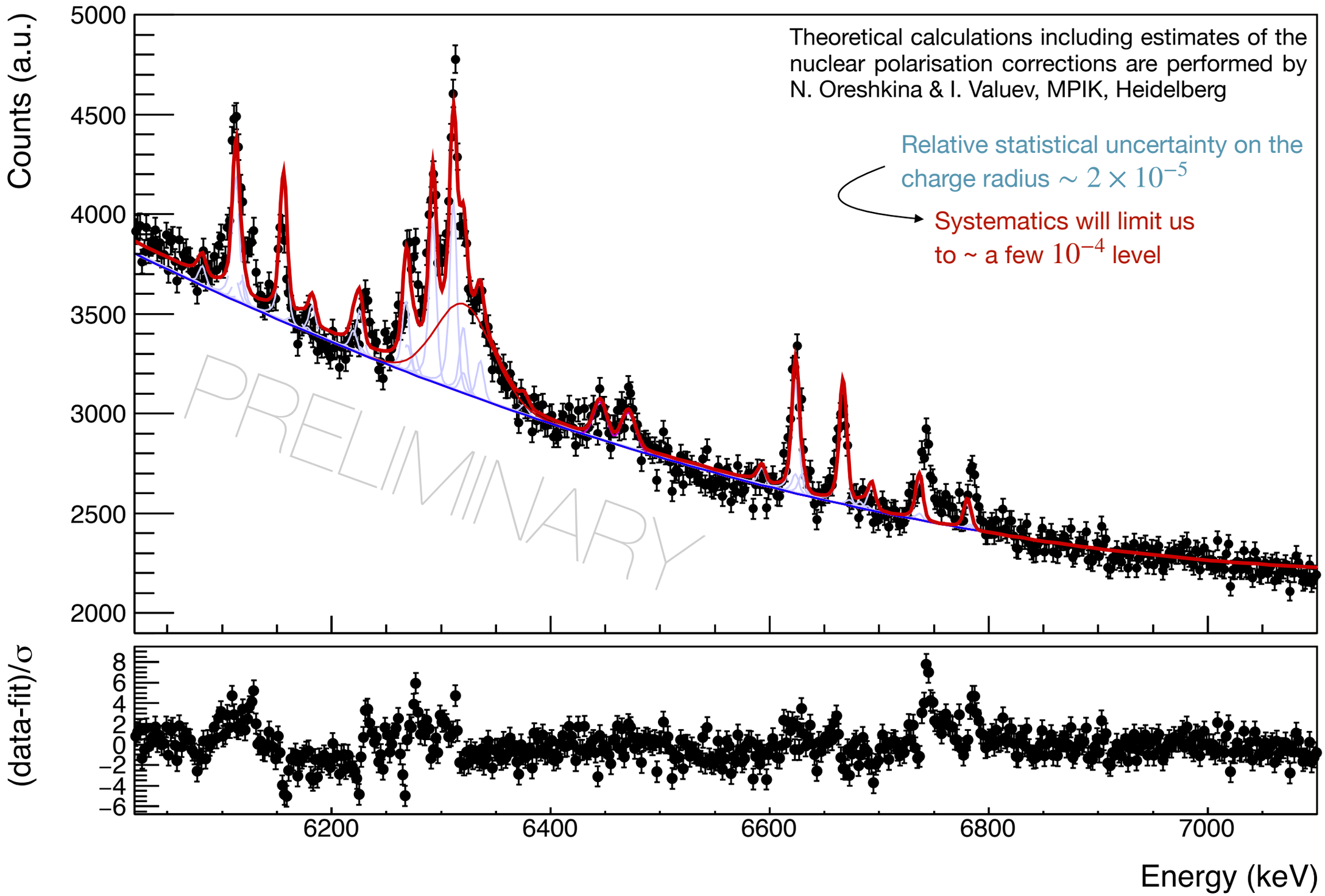

September 2022 measurement

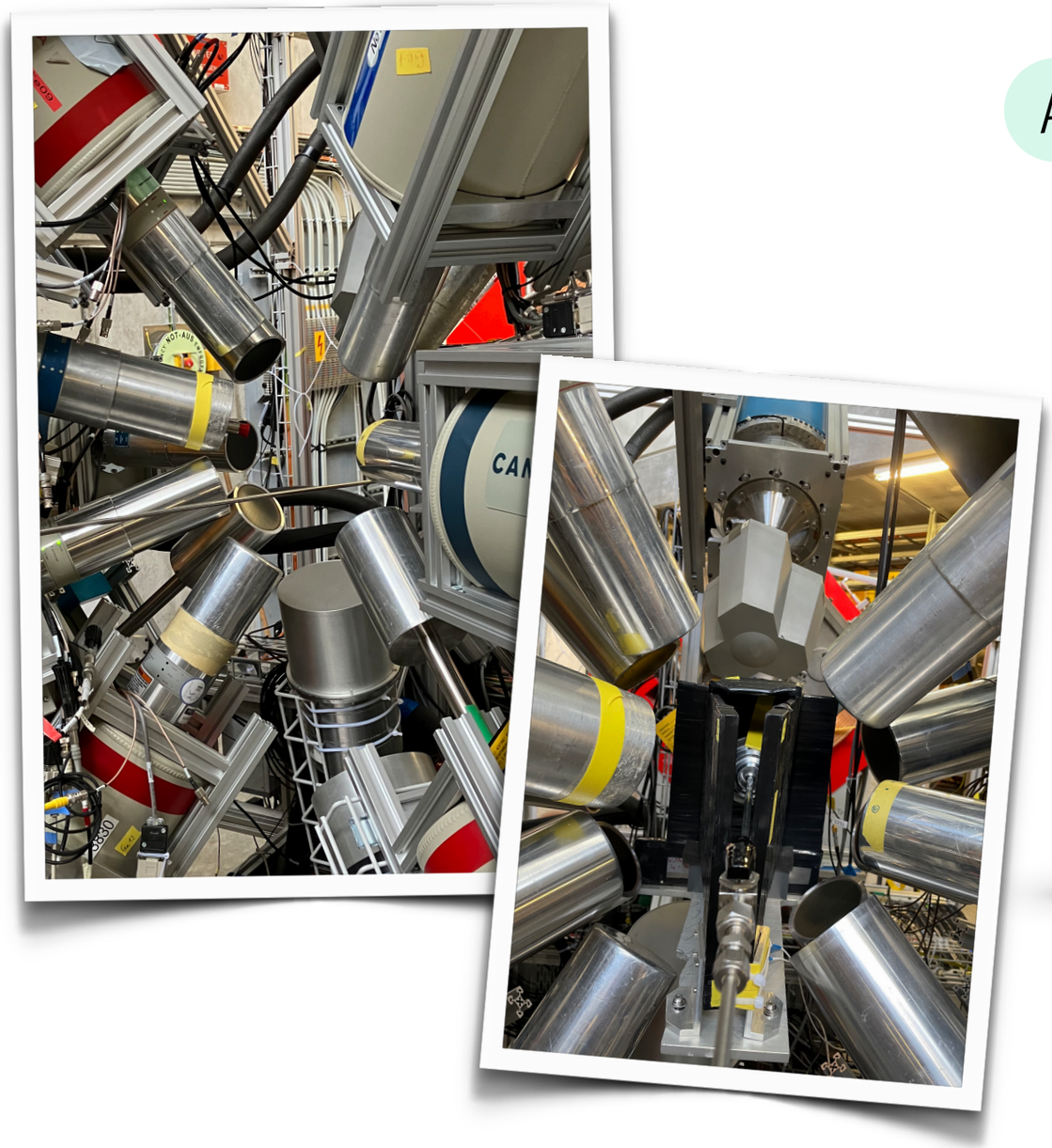

A

Towards the measurement of ^{226}**Ra**:

- measured implanted gold targets
- measured barium deposition targets (drop-on-demand, molecular plating)

B

First **low-Z** elements tests with enriched ^{6}Li and ^{nat}Li samples using a silicon drift detector

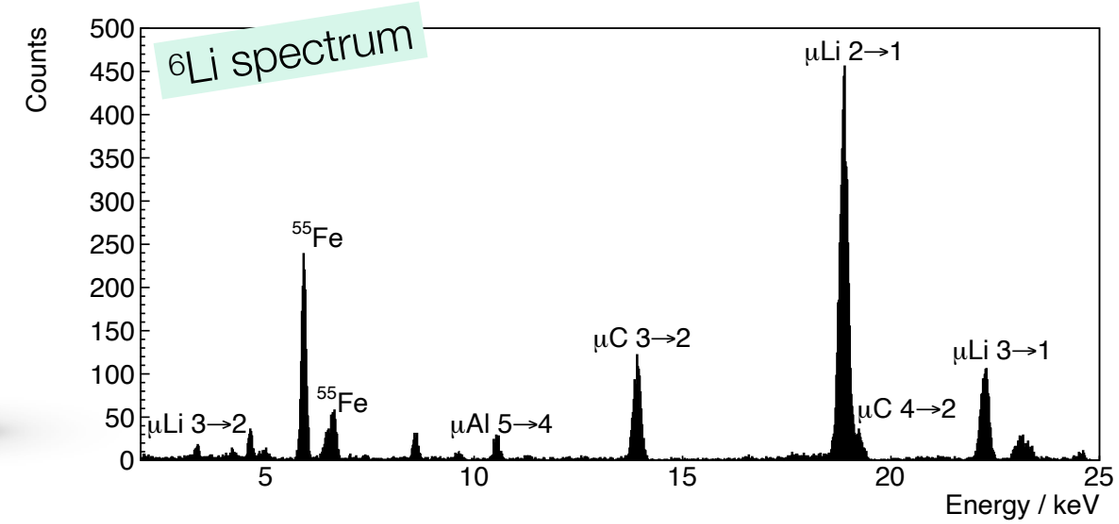

C

Expand towards **medium-Z** elements:

- measured ^{39}K (5.7 μg) using the muX method
- future goal: measure triplet ^{39}K, ^{40}K, ^{41}K
- improve laser spectroscopy results

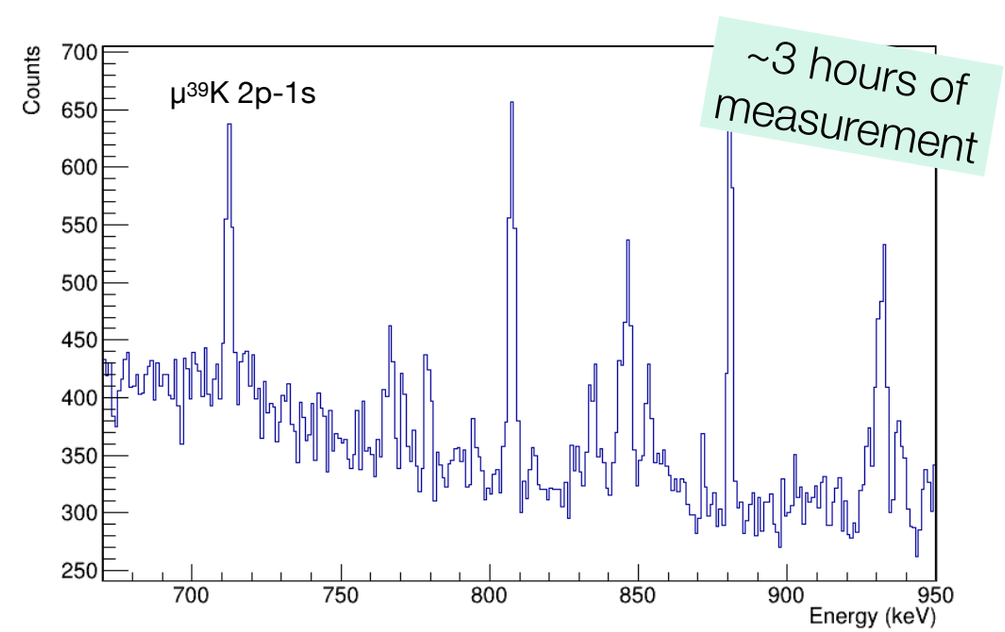

What's next?

- Extraction of the nuclear charge radius of ^{185,187}Re
- Determination of the ^{248}Cm nuclear charge radius
- Remeasure ^{226}Ra

New experimental proposals:

- Measure ^{39}K, ^{40}K, ^{41}K to improve laser spectroscopy results
- Measure low-Z elements (up to neon) using high resolution x-ray detectors to improve the charge radius results

What's next?

- Extraction of the nuclear charge radius of ^{185,187}Re
- Determination of the ^{248}Cm nuclear charge radius
- Remeasure ^{226}Ra

New experimental proposals:

- Measure ^{39}K, ^{40}K, ^{41}K to improve laser spectroscopy results
- Measure low-Z elements (up to neon) using high resolution x-ray detectors to improve the charge radius results

see more on Tuesday 18/10 at 4-5.30 pm

Microcalorimetric high-resolution spectroscopy of muonic lithium	*Katharina von Schoeler*
WHGA / Foyer and Tent, PSI	16:16 - 16:17

What's next?

- Extraction of the nuclear charge radius of ^{185,187}Re
- Determination of the ^{248}Cm nuclear charge radius
- Remeasure ^{226}Ra

New experimental proposals:

- Measure ^{39}K, ^{40}K, ^{41}K to improve laser spectroscopy results
- Measure low-Z elements (up to neon) using high resolution x-ray detectors to improve the charge radius results

see more on Tuesday 18/10 at 4-5.30 pm

Microcalorimetric high-resolution spectroscopy of muonic lithium *Katharina von Schoeler*
WHGA / Foyer and Tent, PSI 16:16 - 16:17

The 2s-1s transition in muonic atoms and atomic parity violation *Frederik Wauters*
WHGA / Foyer and Tent, PSI 16:06 - 16:07

What's next?

- Extraction of the nuclear charge radius of ^{185,187}Re
- Determination of the ^{248}Cm nuclear charge radius
- Remeasure ^{226}Ra

New experimental proposals:

- Measure ^{39}K, ^{40}K, ^{41}K to improve laser spectroscopy results
- Measure low-Z elements (up to neon) using high resolution x-ray detectors to improve the charge radius results

see more on Tuesday 18/10 at 4-5.30 pm

Microcalorimetric high-resolution spectroscopy of muonic lithium *Katharina von Schoeler*
WHGA / Foyer and Tent, PSI 16:16 - 16:17

The 2s-1s transition in muonic atoms and atomic parity violation *Frederik Wauters*
WHGA / Foyer and Tent, PSI 16:06 - 16:07

Thank you!

Backup Slides

Dynamic effect in ^{185}Re

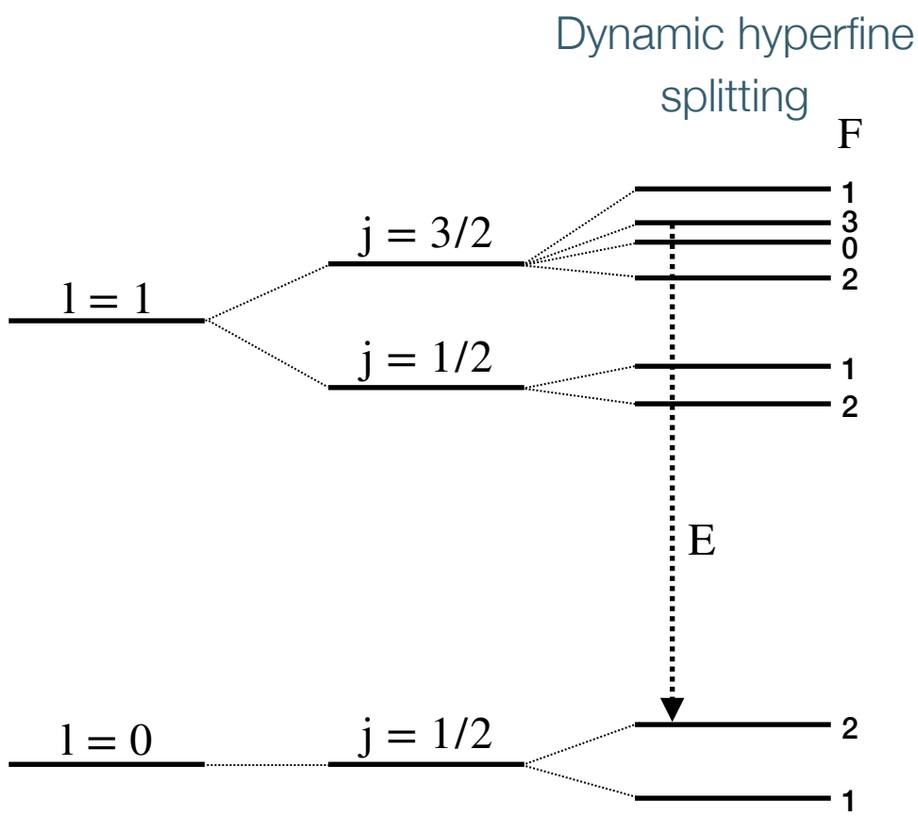

$$I_{\mathbf{ground}} = \frac{5^+}{2}$$

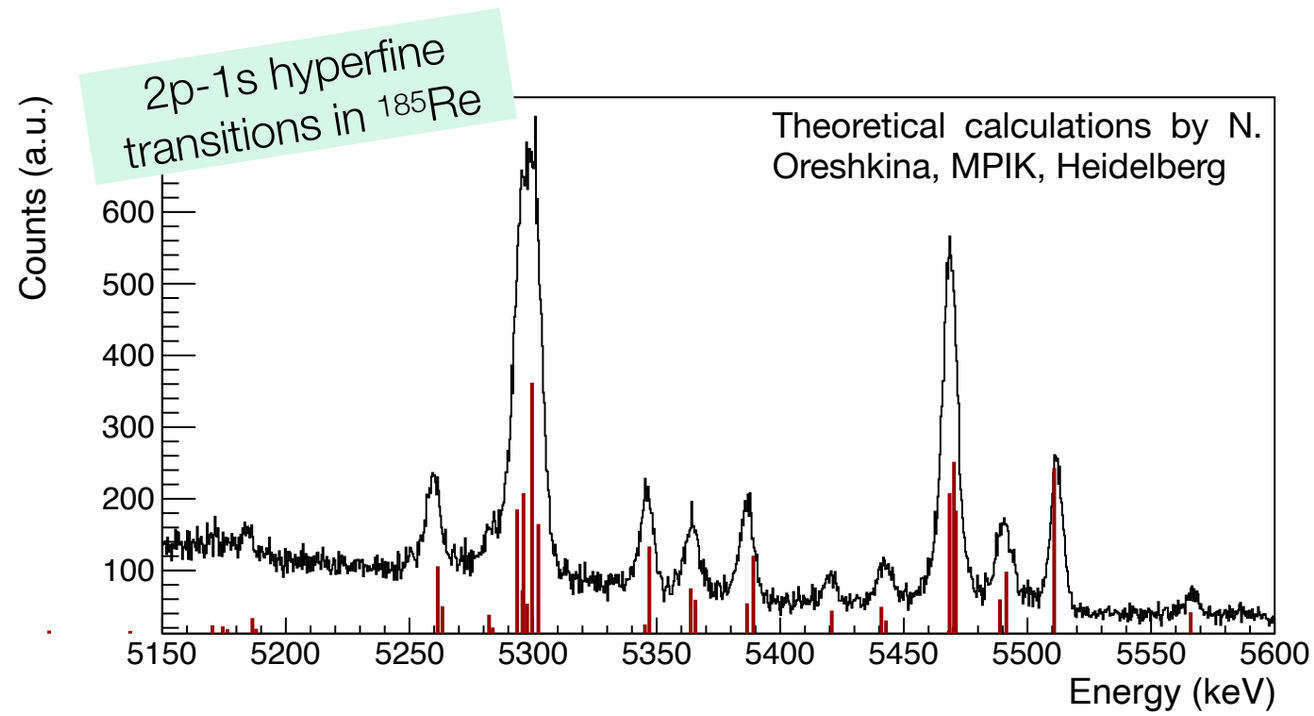

Dynamic effect in ^{185}Re

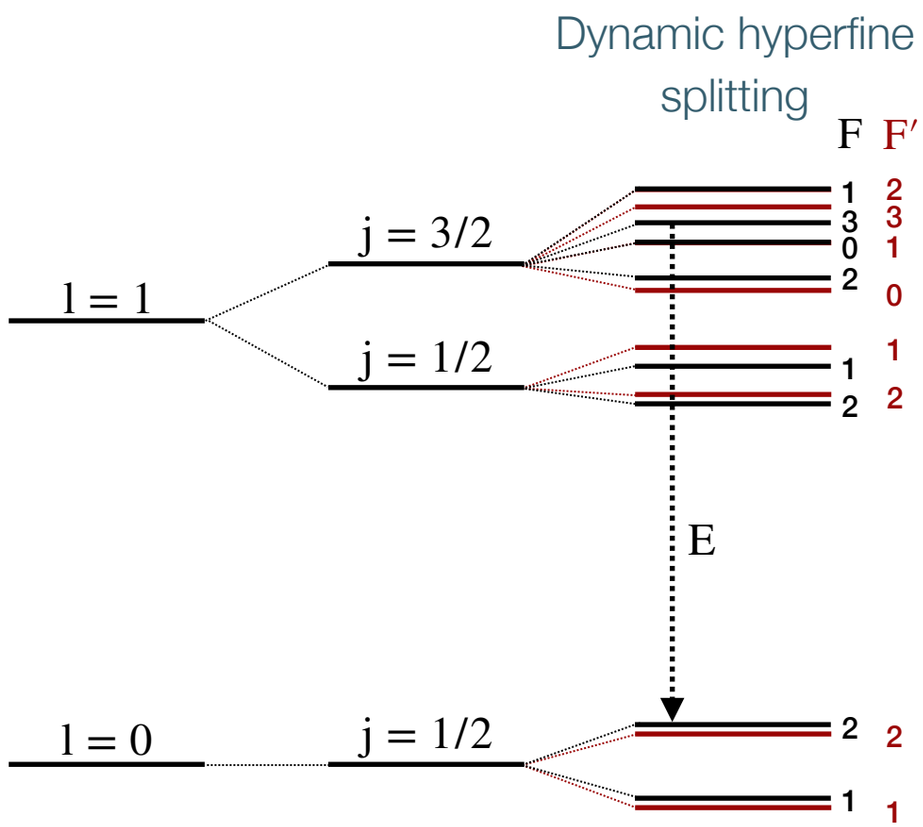

$I_{ground} = \frac{5}{2}^{+}$ $I_{excited} = \frac{7}{2}^{+}$

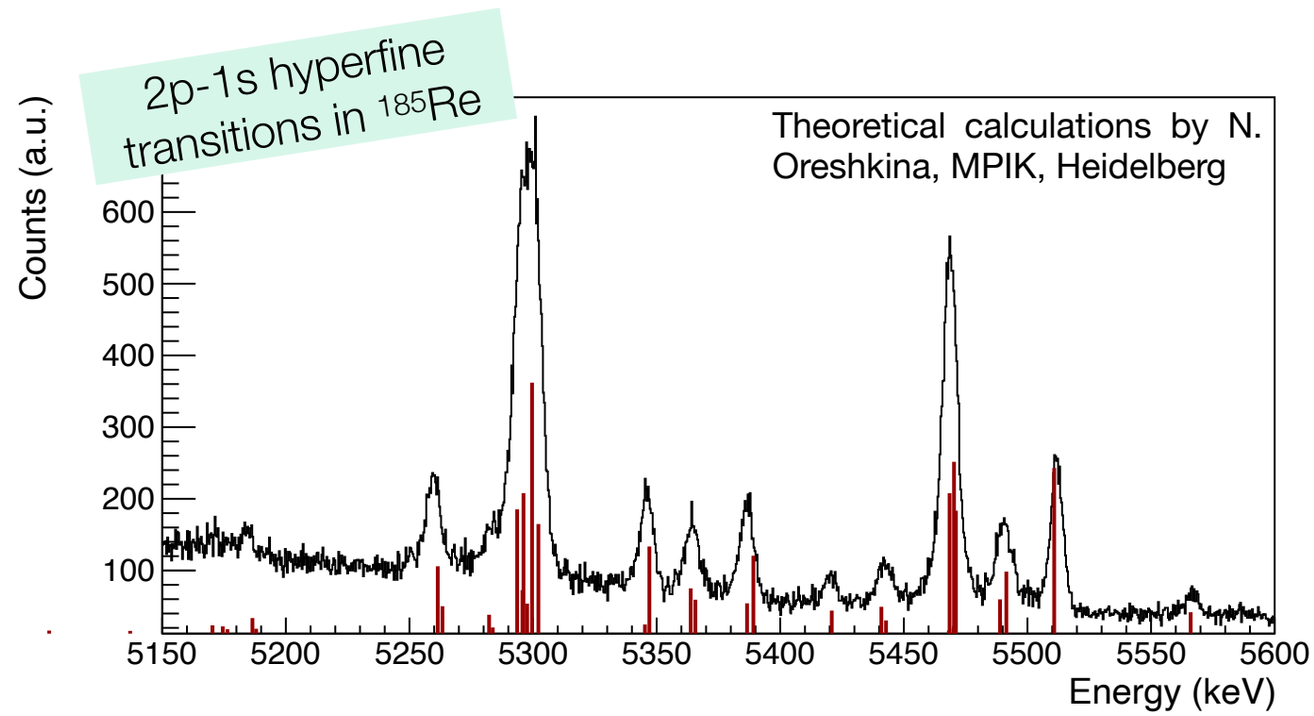

Dynamic effect in ^{185}Re

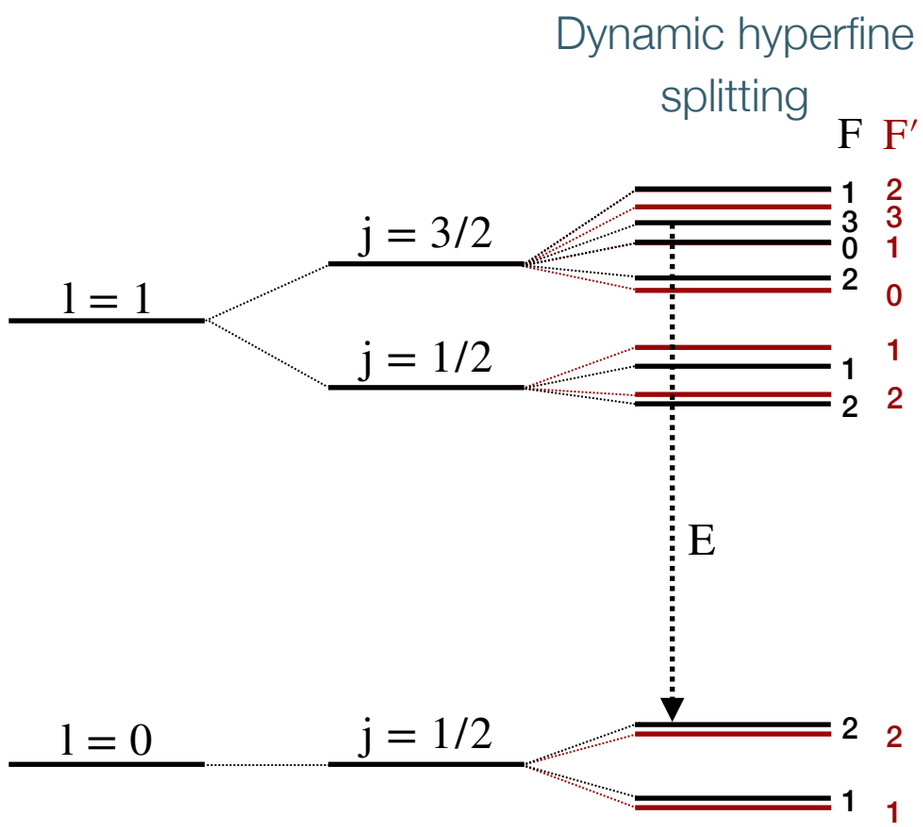

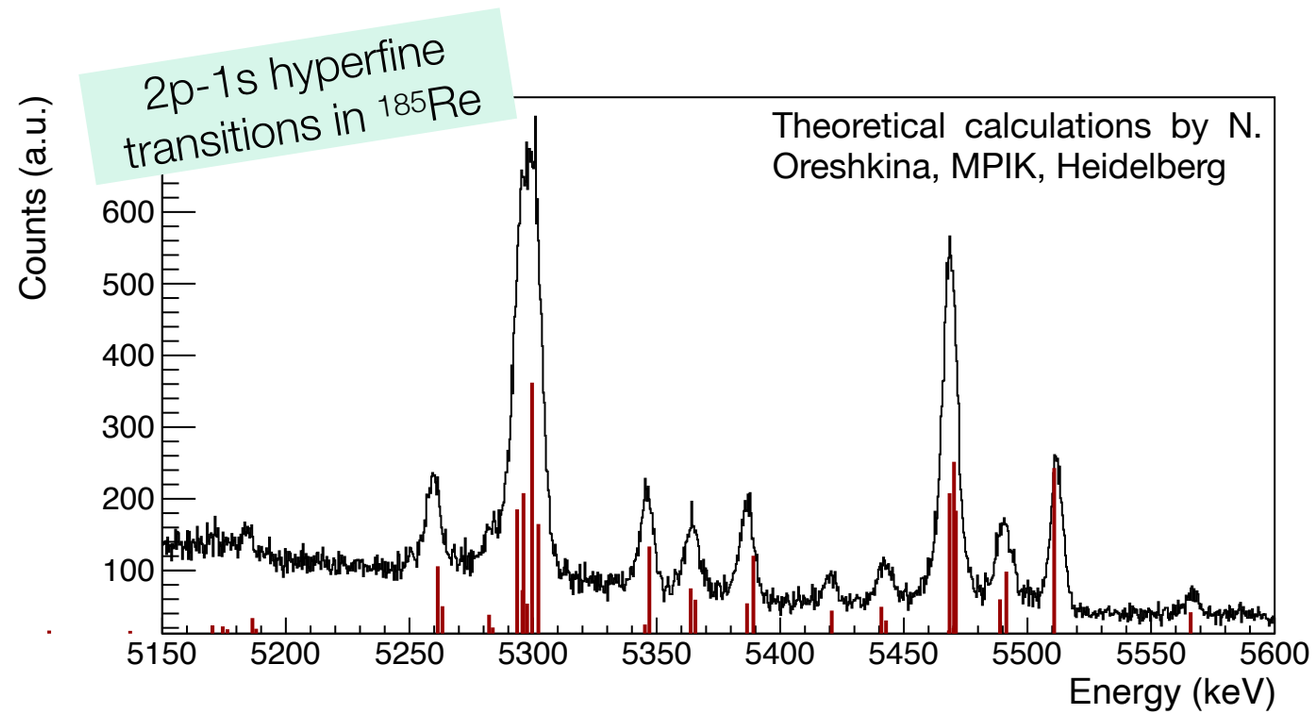

$$I_{\mathbf{ground}} = \frac{5}{2}^{+} \quad I_{\mathbf{excited}} = \frac{7}{2}^{+}, \frac{9}{2}^{+}, \frac{11}{2}^{+}$$

Theory limitations

- Charge radius can be extracted with excellent relative precision
  For ^{208}Pb: $r_C = \langle r^2 \rangle^{\frac{1}{2}} = 5.5031(11)\,\mathrm{fm}$
  $\Rightarrow 2 \cdot 10^{-4}$ relative precision

- Experimental accuracy at the level of ~0.1 keV

TABLE V. Experimental muonic transition energies (keV) in ^{208}Pb (recoil corrected).

Transition	Kessler (Ref. 9)	Hoehn (Ref. 27)	This experiment
$2p_{3/2}$-$1s_{1/2}$	5 962.770(420)		5 962.854(90)
$2p_{1/2}$-$1s_{1/2}$	5 777.910(400)		5 778.058(100)
$3d_{3/2}$-$2p_{1/2}$	2 642.110(60)	2642.292(23)	2 642.332(30)
$3d_{5/2}$-$2p_{3/2}$	2 500.330(60)	2500.580(28)	2 500.590(30)
$3d_{3/2}$-$2p_{3/2}$	2 457.200(200)		2 457.569(70)

- Limitation from theory ⇒ nuclear polarisation effect

- Due to the electrostatic interaction of the muon and nucleus the system is excited to virtual excited states resulting in the increase of the binding energy of the levels

- Limited knowledge of the highly excited nuclear states
  ⇒ nuclear polarisation determines the charge radius accuracy

If nuclear polarisation calculations are improved, more precise charge radius results can be extracted

Phys. Rev. C 37, 2821 (1988)

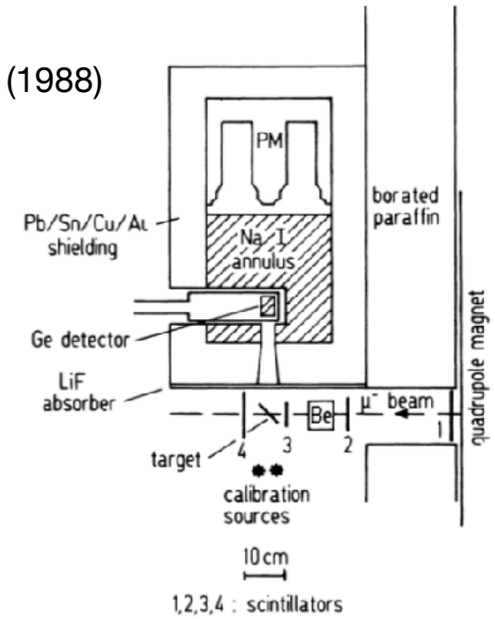

TABLE II. Theoretical nuclear polarization corrections in ^{208}Pb.

Energy (MeV)	I^π	$B(E\lambda)\uparrow$ ($e^2b^{2\lambda}$)	$1s_{1/2}$ (eV)	$2s_{1/2}$ (eV)	$2p_{1/2}$ (eV)	$2p_{3/2}$ (eV)	$3p_{1/2}$ (eV)	$3p_{3/2}$ (eV)	$3d_{3/2}$ (eV)	$3d_{5/2}$ (eV)
2.615	3^-	0.612	135	12	90	84	26	26	111	−63
4.085	2^+	0.318	198	20	182	180	76	84	6	4
4.324	4^+	0.155	14	1	8	7	2	2	1	1
4.842	1^-	0.001 56	7	1	−9	−8	0	0	1	1
5.240	3^-	0.130	27	2	16	15	5	5	2	2
5.293	1^-	0.002 04	9	2	−27	−19	0	−1	1	1
5.512	1^-	0.003 80	16	3	−90	−53	−1	−1	1	1
5.946	1^-	0.000 07	0	0	3	−30	0	0	0	0
6.193	2^+	0.050 5	29	3	22	21	7	7	0	0
6.262	1^-	0.000 24	1	0	3	5	0	0	0	0
6.312	1^-	0.000 22	1	0	3	4	0	0	0	0
6.363	1^-	0.000 14	1	0	2	2	0	0	0	0
6.721	1^-	0.000 75	3	1	6	7	0	−1	0	0
7.064	1^-	0.001 56	6	1	9	11	−1	−1	0	0
7.083	1^-	0.000 75	3	1	4	5	−1	−1	0	0
7.332	1	0.002 04	8	1	10	11	−2	−2	0	0
Total low-lying states			458	48	233	242	111	117	123	−53
13.5	0^-	0.047 872	906	315	64	38	24	15	1	0
22.8	0^+	0.043 658	546	147	43	26	15	10	0	0
13.7	1	0.537 672	1454	221	786	738	255	258	66	54
10.6	2^+	0.761 038	375	37	237	222	67	68	33	30
21.9	2^+	0.566 709	207	21	108	99	29	29	8	7
18.6	3^-	0.497 596	77	7	40	36	11	11	3	2
33.1	3	0.429 112	53	5	25	23	7	7	2	1
	>3[a]		176	15	80	71	21	21	4	4
Total high-lying states			3794	768	1383	1253	429	419	117	98
Total			4252	816	1616	1495	540	536	240	45

[a]Values from Ref. 7. Positive NP values mean that the respective binding energies are increased.

Target production in 2019

Table 1: Summary of all targets produced for the muX beamtime 2019. The given production method ED refers to electrodepostion and DoD refers to drop on demand printing. The maximum allowed quantities in the experimental halle of PSI are 16 μg for ^{248}Cm (given the presence of ^{246}Cm) and 5.5 μg for ^{226}Ra. See text for more details.

Target #	Nuclide	m / μg	A / kBq	Method
Cm-MP2-DoD	Cm-248	15.91	2.50	ED+DoD
Cm-MP3-DoD	Cm-248	15.46	2.43	ED+DoD
Cm-Aceton1	Cm-248	13.72	2.15	DoD (acetone)
Cm-Aceton2	Cm-248	13.94	2.19	DoD (acetone)
Ra-MP1	Ra-226	1.35	49.5	ED+DoD
Ra-MP2	Ra-226	2.50	91.6	ED
Ra-MP3	Ra-226	4.37	160.1	ED+DoD

muX Progress Report 2020 (2019)

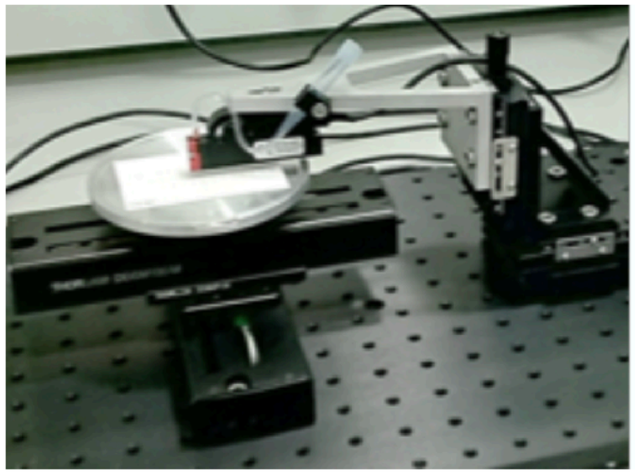

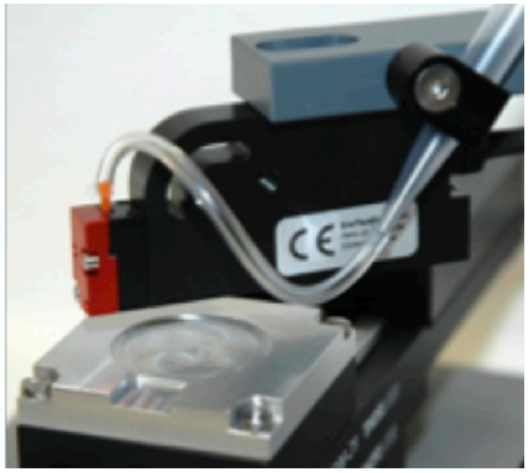

Drop-on-demand printing device at the Johannes Gutenberg-Universitat Mainz

Neutron background

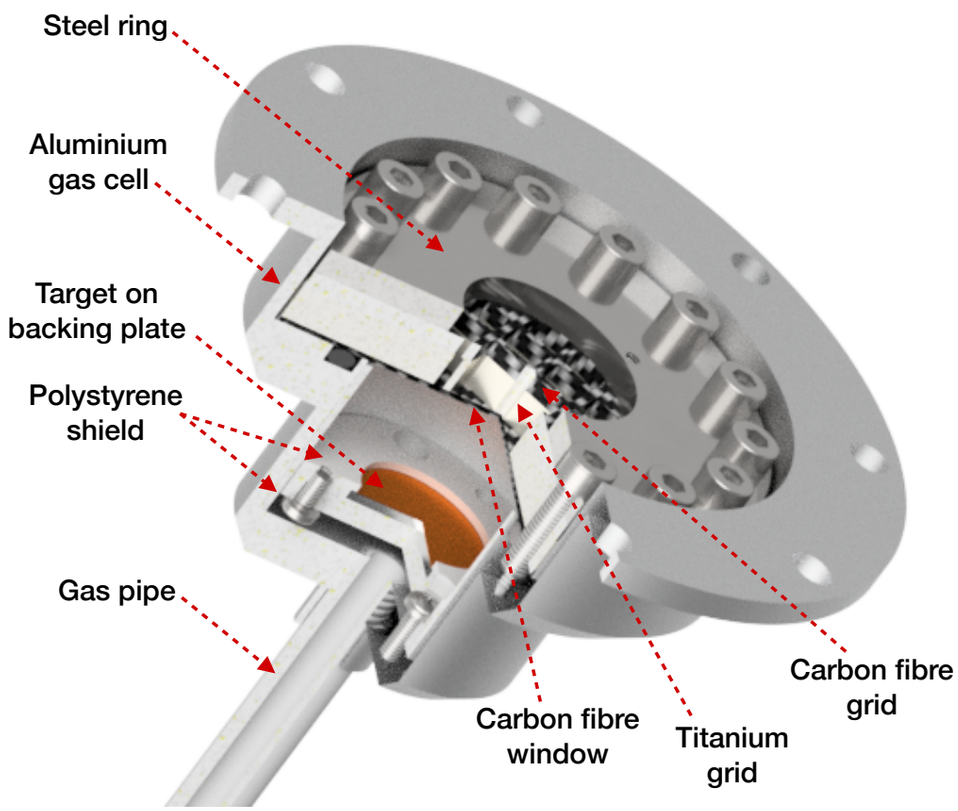

- Another source of background at ~6 MeV: neutrons emitted during the nuclear capture of the muon e.g.

$$\mu^- + (N,Z) \rightarrow (N+1,Z-1)^* + \nu_\mu$$
$$(N+1,Z-1)^* \rightarrow (N,Z-1)^* + n$$

- Those neutrons interact with the Ge crystal and create a continuous background of negative slope
- Effort for only low-Z material in the gas cell

Beam time	2018	2019
Target backing material	copper	glassy carbon
Polystyrene shileding	No	yes

muX Progress Report 2020 (2019)

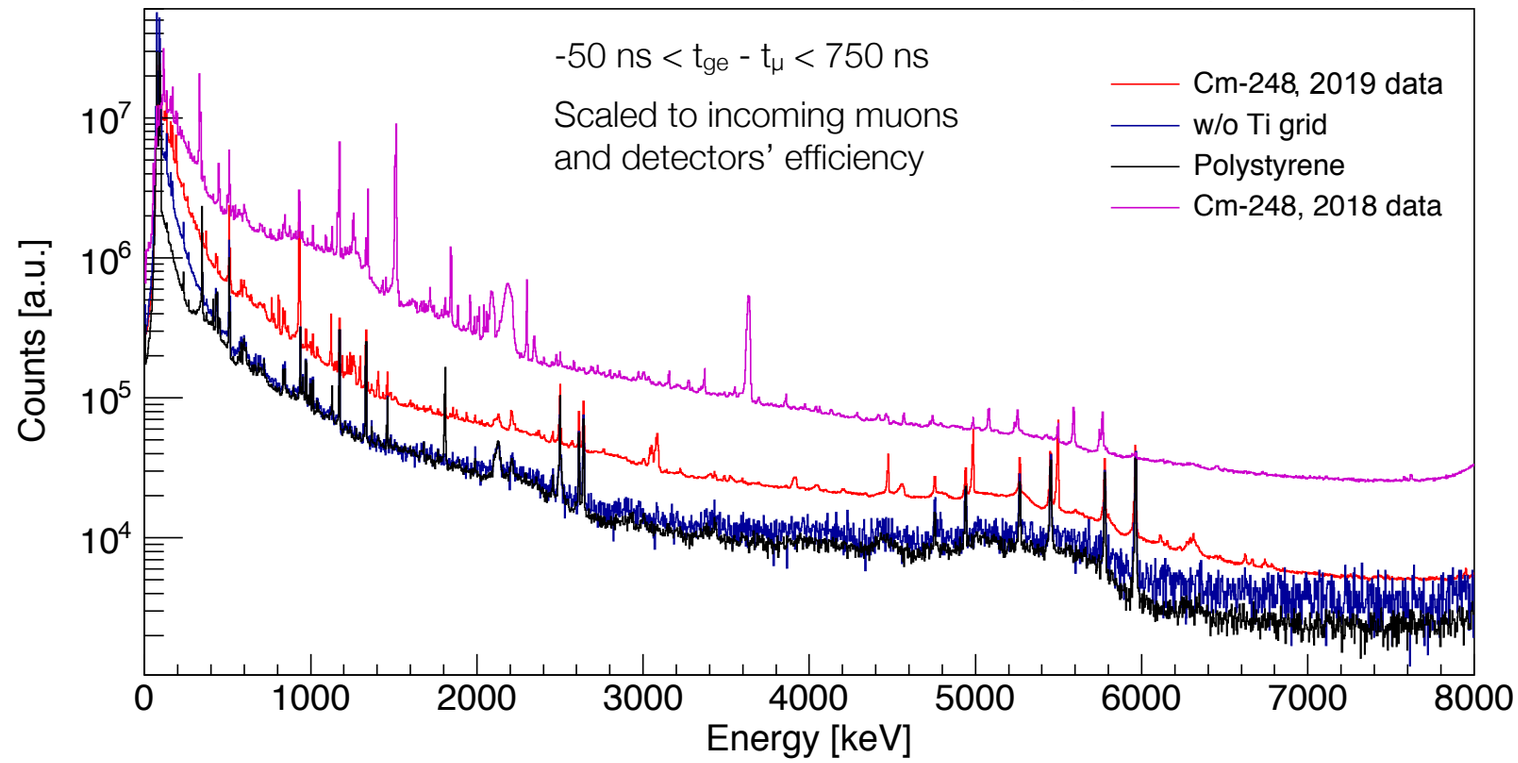

Optimisation of the x-ray yield using a gold target

PhD thesis of A. Skawran
Simulations by J. Nuber

- A 0.2 mg Au target was mounted inside the gas cell
- The amount of the 2p-1s μAu x rays was measured by scanning the:
  - cD → D_2 admixture in H_2 gas (cD)
  - p → stopping position of the muon beam

  - *Maximum yield for 27.25 MeV/c & 0.25% D_2*
  - *Measurements and simulations are in good agreement*

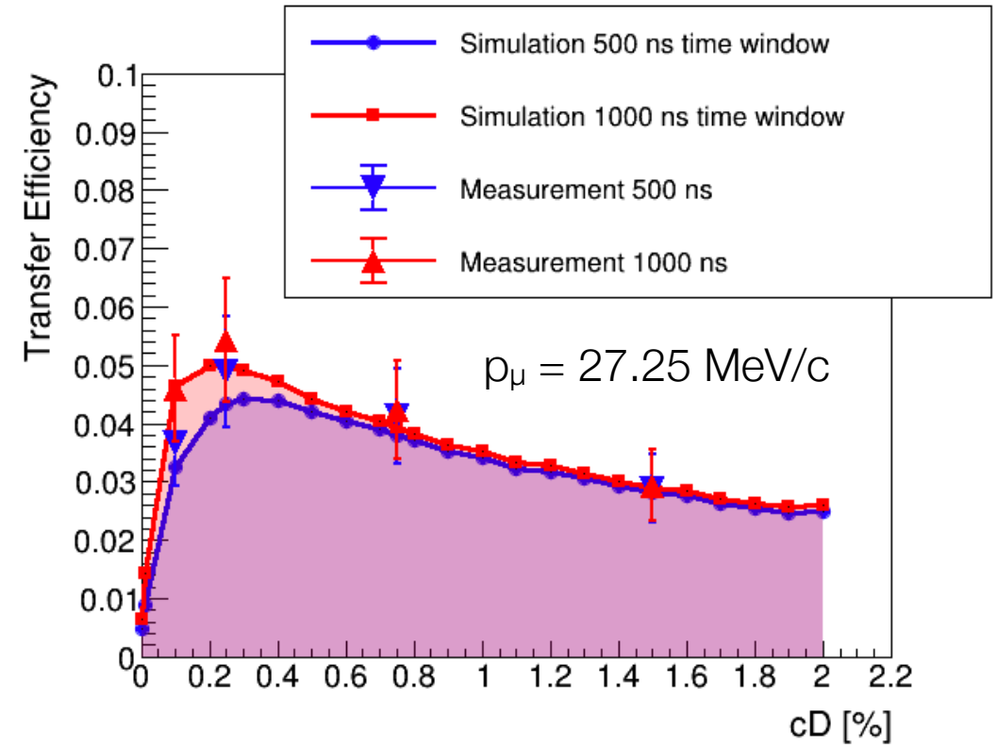

- The time distribution of the observed $2p_{1/2}$-$1s_{1/2}$ gold x ray after transfer for different D_2 concentrations was simulated